Ecological Modelling 440 (2021) 109417

Contents lists available at ScienceDirect

Ecological Modelling

journal homepage: www.elsevier.com/locate/ecolmodel

Primary Research Article

Adapting a dynamic vegetation model for regional biomass, plant biogeography, and fire modeling in the Greater Yellowstone Ecosystem: Evaluating LPJ-GUESS-LMfireCF

Kristen D. Emmett [a,*], Katherine M. Renwick [a,b], Benjamin Poulter [a,c]

[a] Department of Ecology, Montana State University, Bozeman, MT 59717, United States
[b] USDA Forest Service, Northern Region, Missoula, MT 59804, United States
[c] NASA Goddard Space Flight Center, Biospheric Sciences Laboratory, Greenbelt, MD 20771, United States

ARTICLE INFO

Keywords:
Fire modeling
Stand-replacing crown fires
Plant biogeography
Biomass turnover
Ecosystem modeling
Yellowstone National Park

ABSTRACT

North American forests are threatened by changes in climate and disturbance dynamics. Current efforts to model future vegetation and fire dynamics are challenged by the lack of mechanistic representation of ecological processes, the spatial resolution to capture landscape-level heterogeneity, and the ability to model regional spatial extents. To address these gaps, a dynamic vegetation model was adapted for regional applications to the western forests of the U.S. Here we present LPJ-GUESS-LMfireCF, a dynamic vegetation model that includes the ecological processes of a dynamic global vegetation model with cohort-based forest demography (LPJ-GUESS) and a mechanistic fire module (LMfire), with a newly developed routine to simulate stand-replacing crown fires (CF). The LMfireCF fire module calculates surface fire and canopy characteristics to determine if critical conditions are met for crown fire initiation and spread, and if met, calculates crown fire effects. Adapting the model to regional applications required parameterization of dominant regional plant functional types (PFTs) and additional model adjustments related to the representation of fire. Simulations driven by historical climate data from 1980 to 2016 were made to compare the two different fire modules: the original GlobFIRM and newly created LMfireCF, and two different plant functional type (PFT) parameterizations: the original global vs. newly created regional PFTs. Model performance was evaluated by comparing simulation outputs to field and satellite-based estimates for landscape biomass distribution, dominant plant cover, fire activity, and forest regeneration. LPJ-GUESS-LMfireCF accurately represented vegetational zones with elevation and climate gradients in Yellowstone National Park (YNP). Total carbon in aboveground live vegetation within YNP simulated by LPJ-GUESS-LMfireCF with the regional PFTs overestimated satellite-based estimates by 12% (44.8 TgC vs 39.9 TgC respectively). In comparison, an LPJ-GUESS simulation using the older GlobFIRM fire module and global PFTs resulted in total carbon in aboveground live vegetation of 225 Tg C for YNP, five times the satellite-based estimates. LPJ-GUESS-LMfireCF simulated burned area and fire severity approximated satellite-based observations. Importantly, LPJ-GUESS-LMfireCF simulated the large stand-replacing fires of 1988 in Yellowstone as emergent results without model initialization of vegetation cover or fire history. LPJ-GUESS-LMfireCF simulated that 25% of the area of YNP burned in 1988, compared to 36% based on field and satellite-based estimates. However, modeled postfire regrowth was more rapid than field-based estimations, with simulated mean biomass 24 years postfire (40.1 $\pm$ 1.65 Mg ha^{-1}) 58% greater than field estimations (25.4 $\pm$ 2.5 Mg ha^{-1}), yet simulated mean biomass for mature forests (>100 years old without a major disturbance) was 24% less than field estimations (58.4 $\pm$ 0.8 compared to 76.6 $\pm$ 3.5 Mg ha^{-1}). In summary, LPJ-GUESS-LMfireCF effectively simulates regional crown fire dynamics and vegetation to more accurately model regional biomass, plant biogeography, and fire activity.

* Corresponding author. Phone: (541) 743-5820 Fax: (828) 257-4840.
E-mail address: kristen.emmett@usda.gov (K.D. Emmett).

https://doi.org/10.1016/j.ecolmodel.2020.109417
Received 29 May 2020; Received in revised form 12 December 2020; Accepted 15 December 2020
Available online 29 December 2020

1. Introduction

Changes in regional climate and disturbance characteristics threaten the resiliency and function of forested ecosystems (Turner et al., 2019; Walker et al., 2019), increasing the need for regional modeling of forest and disturbance dynamics (U.S. DOE, 2018). Forest resiliency is defined as the capacity of a forest to absorb change and disturbance and have structure and function persist (Holling, 1973). With increases in fire season length, area burned, and frequency of large fires in the boreal and temperate forests of North America (Dennison et al., 2014; Kasischke and Turetsky, 2006; Westerling, 2016, 2006), there is uncertainty about the resiliency of these forests and their carbon storage (Turner et al., 2019; Walker et al., 2019). In particular, the extent of high-severity fires that kill most or all of the trees across entire stands, referred to here as stand-replacing fires, is increasing (Flannigan et al., 2009; Stephens et al., 2014). The ability to predict future forest resiliency is dependent on the development of process-based simulation models that can represent complex interactions between forest demography, disturbance, climatic factors, and increasing atmospheric carbon dioxide (U.S. DOE, 2018). Therefore, appropriately modeling plant geography, disturbance-driven biomass turnover, and forest regrowth under a changing climate is critical to predicting future changes to forests' persistence and function at a regional scale.

Current common approaches to regional forest modeling are empirical models, individual-based simulation models that are extended to landscape applications, or Dynamic Global Vegetation Models (DGVMs) applied regionally. Empirical modeling, including correlation, regression, and principal component analyses can reveal important climatic and disturbance relationships affecting forest productivity (Emmett et al., 2019; Notaro et al., 2019; Potter, 2019). Yet empirical models are often constrained by the limited number of variables included by the modeler that may fail to capture complicated feedbacks between ecological processes. Also, since empirical models are based on correlative relationships between variables from field or remotely sensed data, they rely on statistical extrapolation to make inferences about conditions or areas not explicitly measured. Individual-based forest landscape models offer high-resolution (e.g. 2 m to 30 m spatial resolution) simulations of forest dynamics (Mladenoff, 2004; Seidl et al., 2012). Individual-based simulation models trade their high-spatial resolution for limited spatial extent, making regional-scale simulations computationally impractical.

In contrast, DGVMs were developed for understanding feedbacks between vegetation dynamics, biogeography, and biogeochemistry (Bachelet et al., 2001; Moorcroft et al., 2001; Sitch et al., 2003) at the regional to global scale. DGVMs are process-based simulation models that represent vegetation dynamics including plant establishment, growth, competition, and mortality. The formulations within process-based models are often more closely based on principles of vegetation dynamics (e.g. canopy scaling based on optimum leaf nitrogen distribution) than on empirical relationships, and therefore are less dependent on statistical extrapolation for novel conditions. They also incorporate physical processes (e.g. soil hydrology) and physiological processes (e.g. photosynthesis, respiration, and carbon allocation) important for representing ecological function. The benefit of adapting a DGVM to regional applications is the inclusion of these vegetation dynamics and ecological processes that interact to determine forest resiliency.

Further development of fire dynamics and forest demography in DGVMs is needed to more accurately represent these interactions (Pugh et al., 2019a; U.S. DOE, 2018; Zhu et al., 2016). To capture the ecosystem responses and interactions between vegetation, climate, and disturbance, DGVMs must include comprehensive and realistic fire modules (Keane et al., 2015). The necessity of fire module development in DGVMs led to the formation of the Fire Modeling Intercomparison Project and remains an area of active research (Hantson et al., 2020, 2016; Li et al., 2019, Rabin et al., 2017). While there have been many advances, improvement is needed in the representation of forest fires that burn the crowns of trees or shrubs killing most or all of the overstory (Pugh et al., 2019a, 2019b), hereafter referred to as stand-replacing crown fires (Agee, 1996; Scott and Reinhardt, 2001). Currently, the prominent DGVMs rely upon surface fire models and empirical fire behavior models which do not include the transition of a surface fire into the canopy, limiting their ability to reproduce and predict stand-replacing crown fires (Chaste et al., 2018; Gavin et al., 2014; Hantson et al., 2016; Lehsten et al., 2016; Li et al., 2012; Rabin et al., 2017).

Advances are also needed in the modeling of forest demography within dynamic vegetation models. DGVMs typically simulate plant functional types (PFTs) representing multiple plant species grouped by their physical, phenological, and phylogenetic characteristics. Process-based simulation models are often initiated and constrained by field or remotely sensed data, prescribing the distribution of PFTs or forest productivity. For example, in the Carnegie Ames Stanford Approach ecosystem model simulations, land cover type was prescribed from satellite imagery, and Moderate Resolution Imaging Spectroradiometer (MODIS) Enhanced Vegetation Index and airborne remotely sensed coarse woody debris were used as inputs to estimate net primary productivity (Potter et al., 2011). While initializing and constraining process-based models with observational data can lead to more realistic simulation results, such approaches fail to demonstrate the emergent properties of the model and thereby reduce confidence in prognostic simulations. Calibrating model parameters for simulated PFTs and represented processes is a necessary step to improve model performance without relying on initialization of plant cover type. For example, improving the representation of high-latitude vegetation in another DGVM, Organizing Carbon and Hydrology in Dynamic Ecosystems, required modification of photosynthesis parameters for each simulated PFT, adjustment of temperature limits to tree distributions, and revised tree mortality calculations (Zhu et al., 2015). These DGVM developments have not yet included crown fire simulations, nor have they been applied to all DGVMs.

The dynamic vegetation model LPJ-GUESS is well suited for regional application because it incorporates the physiological and biophysical processes of a DGVM while simulating cohorts of PFTs to represent forest demography. LPJ-GUESS was developed from the DGVM LPJ (Lund-Potsdam-Jena) (Sitch et al., 2003) which represented PFTs as average populations. The General Ecosystem Simulator (GUESS) version represents vegetation as age-based cohorts, allowing the representation of stand structure and mixed plant composition. Simulating age-based cohorts is an intermediate approach between individual-based and population-based models, adding structural complexity while minimizing computational costs to enable regional to global scale applications (Fisher et al., 2018). In LPJ-GUESS vegetation is simulated in independent patches for each grid cell with plant establishment, growth, and competition represented as mechanistic processes based on first principles and empirical relationships (for detailed model description see [Smith et al., 2001]). Previous regional applications of LPJ-GUESS explored vegetation dynamics and plant biogeography in forests of the Northeastern U.S. (Hickler et al., 2004; Tang et al., 2012) and subregions across Europe (Hickler et al., 2012; Koca et al., 2006; Morales et al., 2007; Smith et al., 2008, 2001). However, to adapt LPJ-GUESS for regional application to western U.S. forest biomes several modifications were needed. Minor model modifications included adjustments to pedotransfer functions and the inclusion of soil parent material data (Section 2.2). Major developments included parameterization of regional PFTs to represent the composition of western forests (Section 2.3). In turn, the carbon allocation scheme was modified to produce more realistic tree heights (Section 2.4) and calculations of PFT-specific tree crown length were added (Section 2.5). Most importantly, the fire module LMfireCF was developed to simulate the stand-replacing crown fires characteristic of many western forests (Sections 2.6 and 2.7). The development history of the DGVMs and fire modules relevant to this

study is shown in Fig. 1.

GlobFIRM, the original fire module commonly used within LPJ-GUESS, represents fire occurrence, size, and effects using semi-empirical approaches for non-ignition limited ecosystems (Thonicke et al., 2001). Fire occurrence is determined daily by whether air temperature, fuel moisture content, and abundance of aboveground litter are above minimum thresholds. Fire size is represented as the fraction of a grid cell burned as a function of fire season length, based on an empirical relationship between length of fire season and area burned. While this approach is intuitive, the simplifications overlook potential feedbacks that could be represented by a more mechanistic approach. For example, fire occurrence does not consider the availability of an ignition source or fuel conditions that may be limiting in some ecosystems. Fire size does not consider any mechanisms for fire spread, thereby all fires for a season will be of the same size regardless of fuel availability and fuel moisture. Fire effects are represented as the fraction of biomass burnt by fire is based on a PFT-specific fire resistance parameter. All burned live and dead biomass is considered entirely combusted and added to the annual carbon flux to the atmosphere. This representation of fire effects ignores any varying resistance to fire based on age class and fails to distinguish partially burned (e.g. standing dead, woody debris) and combusted fuels (emitted to the atmosphere).

To better represent fire occurrence, size, and effects in LPJ-GUESS simulations, we integrated LMfire, a mechanistic fire module originally developed for use in LPJ (Pfeiffer et al., 2013). LMfire simulates fire occurrence, behavior, and impact from a more mechanistic perspective by incorporating fire danger indices with fire spread modeling (Pfeiffer et al., 2013; Thonicke et al., 2010). Fire occurrence is based on calculated probabilities of natural ignitions and anthropogenic burning habits. Instead of having fire size based on an empirical relationship with fire season length as in GlobFIRM, LMfire represents fire behavior by calculating fire rate of spread based on weather and topography, following Rothermel's equations (Rothermel, 1972). It also allows multi-day burning and coalescence of fires within patches, more realistically representing fire behavior. However, it must be noted that patches are simulated independently, so fire does not spread between patches or grid cells. Tree mortality is a function of crown scorch and cambial damage based on the current tree height and bark thickness for each PFT.

Simulating stand-replacing crown fires necessitated new developments to the LMfire module, now termed LMfireCF, to represent crown fire (CF), resulting in the ecosystem model variant LPJ-GUESS-LMfireCF. LMfireCF assesses if critical conditions are met for crown fire initiation and spread. Crown fire initiation is dependent on surface fire intensity resulting in a scorch height that reaches the canopy base height. Crown fire spread depends on average canopy bulk density and canopy foliar moisture content meeting critical thresholds.

The purpose of this paper is to introduce LPJ-GUESS-LMfireCF designed for regional application for western forests of the U.S. and to evaluate the model's performance based on regional PFTs and the new fire module. Simulations were run to compare two different fire modules: GlobFIRM and the newly developed LMfireCF. To compare the different potential PFTs, simulations were run with the global PFTs and the newly parameterized regional PFTs. LPJ-GUESS-LMfireCF performance was evaluated for simulated 1) landscape biomass distribution, 2) dominant plant cover distributions, 3) fire activity, and 4) postfire forest regeneration by comparing simulated results to field and satellite-based metrics. Simulations of Yellowstone National Park (YNP) vegetation and wildfire dynamics are used here to demonstrate the utility of LPJ-GUESS-LMfireCF for regional applications in U.S. western forests. YNP serves as a model forested landscape to study the interactions of vegetation, climate, and disturbance dynamics because large stand-replacing crown fires have played an important role in dictating vegetation patterns since the Holocene (Whitlock et al., 2003). The 1988 Yellowstone fires burned about one third of the area of YNP, serving as a natural experiment and validation for fire models.

2. Materials and methods

2.1. Study area

Yellowstone National Park is part of the U.S. Rocky Mountains (Fig. 2). YNP extends 8983 km^2 with a mean elevation of ~2400 m and an elevation range from 1610 m to 3462 m. Long, cold winters and cool summers characterize the climate of YNP (boreal cool summer under the Koppen-Geiger climate classifications, (Kottek et al., 2006)). The northern half of the park experiences warmer mean annual temperatures and lower annual precipitation relative to the southern half (Fig. 3). Vegetation distribution patterns (Fig. 4) correspond to elevation gradients and dominant soil type (Despain, 1990). Volcanic soils are the primary soils in YNP, with relatively nutrient-poor rhyolitic and andesitic soils (i.e. inceptisols) as the most dominant (47%, (Rodman et al., 1996). Mollisols have a higher nutrient and organic matter content and cover 22.3% of the park. The remainder of YNP is covered by combined inceptisols and mollisols (6.4%), bedrock and some soil (8.6%) and thermal soil (2.3%). Areas with inceptisols in the park tend to be dominated by lodgepole pine (*Pinus contorta*) forests while areas with mollisols tend to be nonforested. At lower elevations, forests are comprised of Douglas-fir (*Pseudotsuga menziesii*), Rocky Mountain juniper (*Juniperus scopulorum*), and quaking aspen (*Populus tremuloides*), and nonforested areas are comprised of grasslands and sagebrush (*Artemisia* spp.) steppe. The subalpine areas are dominated by lodgepole pine, with occurrences of subalpine fir (*Abies lasiocarpa*) and Engelmann spruce (*Picea engelmannii*) in the understory or in the canopy in the absence of fire, and limber pine (*Pinus flexilis*) on calcium-rich soils. Higher elevation forested areas are often dominated by whitebark pine (*Pinus albicaulis*). Overall, lodgepole pine dominates more than 80% of the forested area within YNP.

Wildfire often drives vegetation dynamics in YNP, with large high-severity fires that kill most of the trees and initiate secondary succession occurring in the subalpine forests every 150–300 years pre-European settlement (Higuera et al., 2011; Romme, 1982). Fire severity is defined here by the loss of aboveground vegetation and soil organic matter (Keeley, 2009; Ryan and Noste, 1985), with a focus on tree mortality. Lower elevation Douglas-fir forests had low-severity fires with a historical frequency of every 25–60 years (Littell, 2002), with

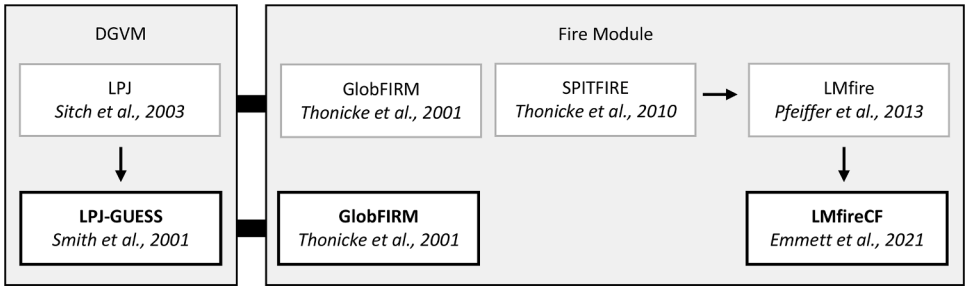

Fig. 1. Schematic showing the development history of dynamic global vegetation models (DGVM) and their fire modules relevant to this study, with references in italics. Arrows indicate development direction from origin to newer derivative. Bold indicates the model and fire modules used for simulations and compared in this study. This paper presents LMfireCF development. (For interpretation of the references to colour in this figure legend, the reader is referred to the web version of this article.)

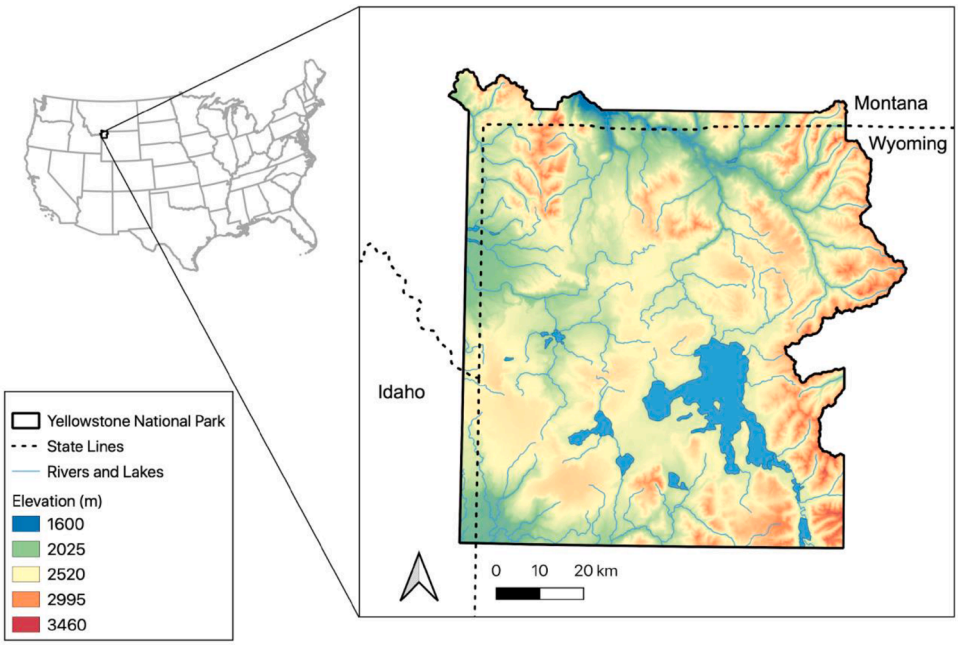

Fig. 2. Map of Yellowstone National Park (YNP) showing elevation (m) based on the STRM 90 m digital elevation model with rivers and lakes displayed in blue. YNP is located in the northwest corner of the state of Wyoming in the U.S. (For interpretation of the references to colour in this figure legend, the reader is referred to the web version of this article.)

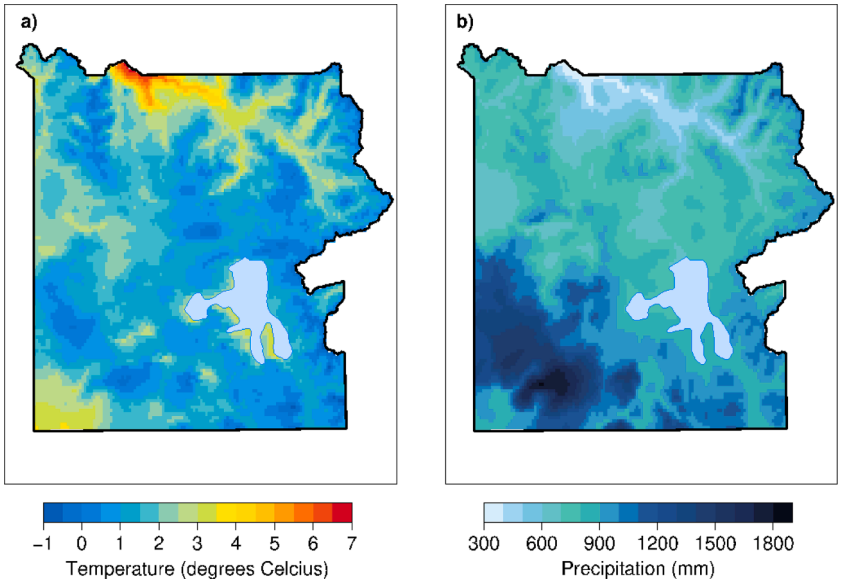

Fig. 3. Climatological mean distributions during the study period 1980–2016 across Yellowstone National Park of a) mean annual temperature (degrees Celsius) using TopoWx v1.3.0 (Oyler et al., 2015) and b) mean annual precipitation (mm) using Daymet v 3 (Thornton et al., 2017).

shorter 30 year mean fire frequency in shrub and grasslands (Barrett, 1994). Higher elevation whitebark pine forests had high to mixed severity fires with a mean fire return interval of over 350 years (Barrett, 1994).

A policy of complete fire suppression was in effect since the park was founded in 1872 up to 1972 (Romme and Despain, 1989). Yet efforts were not effective until about 1945 when modern fire-fighting technologies became available. This relatively short period of effective fire suppression is unlikely to have greatly influenced fire activity (Romme and Despain, 1989). The fires of the late twentieth century are considered comparable to fires in the early 1700s, except that the vast majority of the area burned in one year, 1988 (Romme and Despain, 1989). The historic fires of 1988 burned about 36% percent of the park and left a landscape mosaic of unburned areas and burned areas with varying burn severity (Turner et al., 1994). Large fire years, including 1988, were associated with extreme weather conditions characterized by hot and dry summers and strong winds (Bessie and Johnson, 1995; Renkin and Despain, 1992; Westerling et al., 2011).

2.2. Model and simulation descriptions

LPJ-GUESS v. 2.0 was used for simulations in this study; the physiological and biophysical processes are from LPJ (Sitch et al., 2003) and other model details are given by Smith et al. (2001), except for the model developments described in this paper. LPJ-GUESS tracks characteristics of an average individual for each age-based cohort of tree and

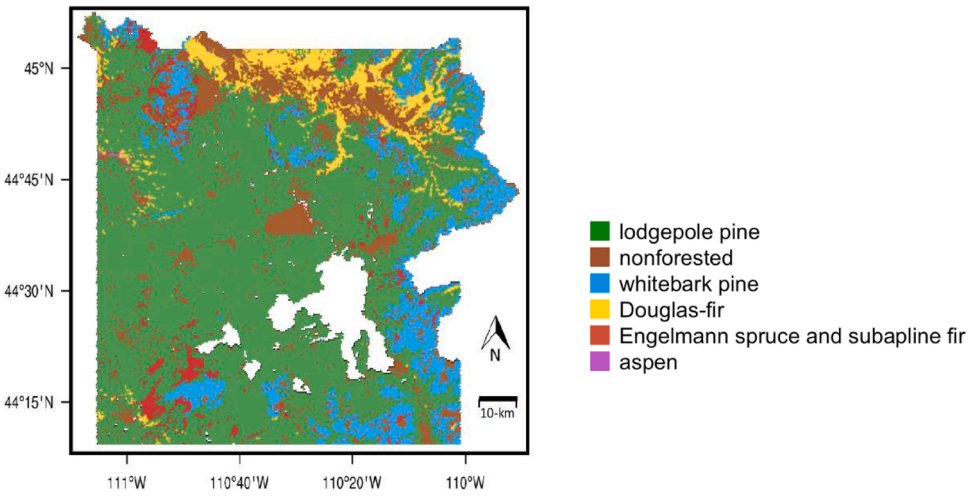

Fig. 4. Map of primary vegetation type using the National Park Service (NPS) Yellowstone 1999 Cover Type dataset, provided by the NPS and based on color aerial photography and field surveys (reproduced with permission from Notaro et al., 2019 Remote Sensing).

shrub PFTs, making the assumption that individuals of the same age in the patch have the same structure. Tree structure is simplified to a crown cylinder with assumed uniform distribution of carbon. Each grass PFT is represented as a single individual.

LPJ-GUESS simulates dynamic vegetation in patches for each grid cell. Patches share environmental input values of the grid cell, termed replicate patches, but run independently to represent the variability of stochastic processes: establishment, background mortality, and fire. The exception is that patches are assumed to share a common propagule pool (i.e. spatial mass effect [Shmida and Ellner, 1984]). Initially, propagules are assumed to be available for a PFT if the climatic conditions are met in the grid cell. After colonization, establishment of new PFT saplings is dependent on the reproductive output of all cohorts of that PFT in the previous year. The number of saplings established per unit area per year is drawn from a Poisson distribution, limited by the set maximum for that PFT (parameter 'est_max' (saplings/m^2/year)), to represent stochastic establishment. Variables are output as averages for the patches within a grid cell.

A coupled photosynthesis and hydrology module calculates plant carbon uptake limited by photosynthetically active radiation and stomatal conductance (Haxeltine and Prentice, 1996; Smith et al., 2001). Carbon uptake is also influenced by air temperature relative to temperature optimums and atmospheric carbon dioxide concentrations. LPJ-GUESS simulates light competition between PFT cohorts based on their crown structure and canopy position using the Lambert-Beer law for attenuation of light through the canopy (Prentice and Leemans, 1990). PFTs also compete for soil water, with uptake dependent on root distribution in the soil (Smith et al., 2001).

Soil hydrology is represented as a "bucket model" (Manabe, 1969) with a two-layer soil profile (Haxeltine and Prentice, 1996). Water infiltrates the upper soil layer (0–0.5 m) through precipitation (minus interception) or melting snow pack. Soil water content is depleted by plant evapotranspiration, percolation below the lower soil layer (0.5–1.5 m), surface evaporation, or if the upper soil layer is saturated, via surface runoff. The calculation of water holding capacity and other soil parameters was modified for this study to allow for the use of continuous soil texture data instead of being limited to nine soil texture classes. The pedotransfer functions follow Cosby et al. (1984), with volumetric water holding capacity equal to the field capacity minus the water holding capacity at wilting point (Appendix D, Fig. D2).

For this study, Yellowstone National Park was simulated as a landscape of 14,431 1km^2 grid cells using LPJ-GUESS (Cartesian area). LPJ-GUESS simulations were run by repeatedly selecting a year randomly from detrended historical Daymet climate data (1980–2016) and static carbon dioxide concentrations (1860 value, 286.4 ppm) for 1000 years (called a "spin-up"), which is required for LPJ-GUESS to establish soil carbon pools and for simulated vegetation to reach theoretical equilibrium with average climate. Each grid cell was run with 10 replicate patches to represent differences in stand structure and PFT composition resulting from stochastic processes. Simulations were then run for 157 years (1860–2016) with transient atmospheric carbon dioxide data for years 1860–2016, detrended climate data for years 1860–1989, and historical climate data for years 1980–2016. Simulations were run to compare the different fire modules (GlobFIRM and LMfireCF) and different PFTs (global PFTs and the new regional PFTs). PFTs are listed in Table 2 and described in the following section. While an LPJ-GUESS-LMfire (crown fire routine disabled) simulation for the entire YNP was not included in this study, diagnostic plots comparing LMfire and LMfireCF were included in Appendix F.

2.3. Regional PFT parameterization

To better represent forest demography and crown fire dynamics, we replaced the more general global tree PFTs that are typically used in LPJ-GUESS with species-specific parameterizations for the eight dominant tree species in YNP. Four species: lodgepole pine (*Pinus contorta*), Douglas-fir (*Pseudotsuga menziesii*), quaking aspen (*Populus tremuloides*), and Rocky Mountain juniper (*Juniperus scopulorum*) were parameterized individually. Due to their physical and functional similarities and geographic range overlap (McCaughey and Schmidt, 2001, 1990), whitebark pine (*Pinus albicaulis)* and limber pine (*Pinus flexilis)* were represented as a single high-elevation "5-needle pines" species pair, while Engelmann spruce (*Picea engelmannii)* and subalpine fir (*Abies lasiocarpa)* were similarly represented as a single "spruce-fir" species pair. In addition to these six species/species pairs (hereafter "PFTs"), a sagebrush shrub (*Artemisia* spp.), and two grass PFTs ("cool grass" with C_3 photosynthetic pathway and "warm grass" with C_4 photosynthetic pathway) were parameterized to represent non-forest vegetation (Table 1).

Values, sources, and citations for PFT parameters are included in Appendix A, Tables A1-A4. The bioclimatic limits for establishment and survival were based on two standard deviations below or above the mean values calculated from Daymet climate for the range of a PFT based on the USDA Forest Service's Forest Inventory and Analysis (FIA) presence data (Gillespie, 1999). For PFTs that represent two species, the more extreme bioclimatic values were used to represent a range inclusive to both species, unless otherwise noted in Appendix A, Table A1. Thereby, the bioclimatic limits for Engelmann spruce were used for the

Table 1
Regional plant functional types (PFTs) used for LPJ-GUESS-LMFireCF simulations with three descriptive model parameters. Dominant vegetation was represented as nine PFTs: lodgepole pine (*Pinus contorta*), a spruce-fir (*Picea engelmannii* and *Abies lasiocarpa*), Douglas-fir (*Pseudotsuga menziesii*), 5-needle pines (*Pinus albicaulis* and *Pinus flexilis*), aspen (*Populus tremuloides),* juniper (*Juniperus scopulorum*), sagebrush (*Artemisia tridentata*), a multi-species cool grass (C_3, for the photosynthetic pathway), and a multi-species warm grass (C_4). All PFTs use C_3 biochemical pathway for photosynthesis, except C_4 warm grass. The fraction of annual net primary production used for fruits, seed, and flowers (reprfrac) was set to 0.1 for all PFTs, except for sagebrush which was set to 0.01.

Description & Parameters	PFT								
	Lodgepole pine	Spruce-fir	Douglas-fir	5-needle pines	Aspen	Juniper	Sagebrush	Cool grass	Warm grass
Species represented	*Pinus contorta*	*Picea engelmannii* *Abies lasiocarpa*	*Pseudotsuga menziesii*	*Pinus albicaulis* *Pinus flexilis*	*Populus tremuloides*	*Juniperus scopulorum*	*Artemisia tridentata*	many C3	many C4
Growth form^	tree	tree	tree	tree	tree	tree	shrub	grass	grass
Phenology	evergreen	evergreen	evergreen	evergreen	summergreen	evergreen	semi-deciduous	summergreen	summergreen
Shade tolerance class^^	intolerant	tolerant	intermediate	intermediate	intolerant	intolerant	intolerant	*NA*	*NA*

^ See Appendix A, Table A3. for parameters specific to growth form types.
^^ See Appendix A, Table A4. for parameters specific to shade tolerance classes.

spruce-fir PFT and the limits for whitebark pine were used for the high-elevation 5-needle pines PFT. Plant trait, fuel loading, and post-fire vegetation data were collected for this study spanning foothill to alpine vegetation zones across the Greater Yellowstone Ecosystem (GYE) to parameterize the LPJ-GUESS and the LMfire model (Appendix B). Calibration of PFT parameter values included conducting a sensitivity analysis and comparing adjustments of groups of parameters (e.g. shade tolerance parameters) effect on species dominance. In a grid cell with inceptisol soils, lodgepole pine background and maximum establishment rates were increased. These parameter adjustments served as a proxy for lodgepole pine's improved competition against other tree PFTs in nutrient-poor volcanic soils.

The production of fire-adapted cones that open when exposed to high temperatures, known as serotinous cones, varies amongst populations of lodgepole pines (Schoennagel et al., 2003). Serotiny was not included in LPJ-GUESS-LMfireCF, so all grid cells were assumed to have the same availability of propagules independent of their fire history, not including a critical restraint on lodgepole pine regeneration. The maximum sapling establishment rate (PFT specific parameter 'est_max' (saplings/m^2/year)) for lodgepole pine was set to one tenth the mean stem density 24 years after fire (Turner et al., 2004).

2.4. Carbon allocation modification

A key model development was required for more accurate representation of tree heights. Previously in LPJ-GUESS v. 2.0, the ratio of tree leaf area to sapwood area was based on a PFT-specific constant, or size-independent allocation, retained from LPJ (Sitch et al., 2003, see Eq. (1)). For this study, tree heights were constrained by modifying the allometric relationship between the ratio of tree leaf area and sapwood cross-sectional area to include tree height as a covariate. A size-dependent leaf to sapwood area (*latosa*) ratio was implemented, decreasing the *latosa* parameter value for each PFT cohort (noted by subscripts $_{c,PFT}$) by twenty units per meter increase in tree height (h) based on previous relationships used by McDowell and Zaehle (McDowell et al., 2002; Zaehle et al., 2006):

$$latosa_{c,PFT} = -20{*}h_{c,PFT} + latosa_{PFT} \quad (1)$$

where $latosa_{PFT}$ is the maximum parameter value for a PFT. In turn, this adjusted *latosa* value was then used to constrain height ensuring that each unit of leaf area is supported by an appropriate amount of transport tissue, following the 'pipe' model (Shinozaki et al., 1964a, 1964b).

2.5. PFT crown length

In LPJ-GUESS v. 2.0, crown lengths (tree height minus crown base height) were previously set equal to tree height for all PFTs, and in LMfire, crown length was calculated as 33% of the height for all trees, neither of which are representative of tree growth in GYE species. Instead, in LMfireCF crown length varies with height based on PFT-specific parameters. Linear and quadratic regression equations were fit to field measurements of height vs. crown length for GYE tree species (Appendix B). The linear slope (m) and intercept (b) values were then used to calculate variable crown length (cl) based on tree height (h) in LPJ-GUESS-LMfireCF for each PFT cohort ($_{c,PFT}$):

$$cl_{c,PFT} = m_{PFT}{*}h_{c,PFT} + b_{PFT} \quad (2)$$

Crown base height (cbh), which is used in the LMfireCF module, was then calculated by subtracting the crown length from the tree height:

$$cbh_{c,PFT} = h_{c,PFT} - cl_{c,PFT} \quad (3)$$

2.6. LMfire fire module modifications

Our model improvement included coding the LMfire routines to operate on age-based PFT cohorts in LPJ-GUESS, as opposed to uniformly aged populations (Pfeiffer et al., 2013; Thonicke et al., 2010), enabling representation of mixed-aged stand dynamics. Tree height, diameter, and bark thickness are distinguished for each age-based PFT cohort, so in LPJ-GUESS-LMfireCF fire effects can vary between canopy layers.

Partitioning of carbon pools was based on original LMFire/SPITFIRE values (Pfeiffer et al., 2013; Thonicke et al., 2010), except it was necessary to increase 1 hour fuels from 4.5% (reducing 1000 hr fuels by 0.225%) for regional simulations. The standard fuel size classes based on the diameter of live or dead woody fuels are <0.6 cm 1-hour timelag, 0.6–2.5 cm 10-hour timelag, 2.5–8.0 cm 100-hour timelag, and >8 cm 1000-hour timelag (Baker, 2009). Since simulated vegetation is tracked as amorphous carbon pools (e.g. leaf, sapwood, heartwood), the fuel size classes are calculated as fractions of total live or dead carbon (4.725%, 7.5%, 21% and 66.775% for 1, 10, 100, and 1000 hr fuels respectively).

Combustion of live biomass within a simulated patch is calculated for each PFT cohort and is proportional to the fraction of area burned, fraction of crown scorch, live carbon, and a combustion fraction constant by fuel size class. Combustion fraction constants for live biomass killed by fire were adjusted from 100% of 1 hour fuels and 5% of 10 hour fuels (Chaste et al., 2018; Pfeiffer et al., 2013) to 90%, 80%, 50%, and 0% for 1, 10, 100, and 1000 hour fuels respectively (Keane et al., 2011). The remaining live vegetation killed by fire is transferred to litter.

Fractions of dead biomass combusted depend on fuel moisture content relative to its moisture of extinction by fuel size class. The moisture of extinction is the fraction of moisture content above which fuel stops burning. Moisture of extinction values were adjusted from 0.404, 0.487, 0.525, 0.5440 for 1, 10, 100, and 1000 hour fuels respectively (Pfeiffer et al., 2013) to 0.2 for all fuel size classes based on estimates that the moisture of extinction rarely exceeds 15–30% (Scott and Burgan, 2005). Other parameter values for the LMfireCF fire module are shown in Appendix C, Table C1.

2.7. Crown fire dynamics

A newly developed routine to simulate stand-replacing crown fires (CF) was incorporated with LMfire and in addition to the modifications described previously, result in the fire module LMfireCF. In LPJ-GUESS-LMfireCF, to determine if crown fires (*CF*) would occur in a patch, surface fire and canopy characteristics were calculated to determine if critical conditions were met for crown fire initiation (*CFI*) and crown fire spread (*CFS*):

$$CF = \begin{cases} 1, & if\ CFI = 1\ and\ if\ CFS = 1 \\ 0, & otherwise \end{cases} \quad (4)$$

Crown fire initiation requires a critical surface fire intensity for the start of crowning, such that the scorch height reaches the canopy base height (Van Wagner, 1993, 1977). Scorch height (*SH*) is calculated as,

$$SH = 0.148 * I^{2/3} \quad (5)$$

where I is surface fire intensity (kW m^{-1}) (Alexander, 1982; Van Wagner, 1973). The constant modifier was set at 0.148 as found by Van Wagner (1973) an increase from the 0.094 assigned by Pfeiffer et al. (2013).

Since LPJ-GUESS represents age-based cohorts of PFTs, canopy bulk density was calculated for each horizontal canopy layer that was 1 m thick (≥0.5 m) to determine canopy base height, canopy height, and average canopy bulk density. Canopy bulk density is the sum of leaf and 1-hour live fuel mass per unit volume of canopy, as this is considered the biomass that would burn quickly to sustain crown fire spread (Brown et al., 1991; Keane et al., 2005; Reinhardt et al., 1997; Scott and Reinhardt, 2001). In the following equations, lowercase annotations are used for age-cohort crown variables and uppercase annotations are used for forest canopy variables. Assuming crown bulk density (*cbd*) is uniform throughout the crown length (*cl*) for the average individual representing each PFT cohort (*c,PFT*), leaf biomass and 1-hour live fuel biomass (*lf (class)*) were averaged for each crown layer (*l*) from crown base height (*cbh*) to tree height (*h*):

$$cbd_{l,c,PFT} = \sum_{l=cbh}^{h} \frac{leafbiomass_{c,PFT} + lf(1)_{c,PFT}}{cl_{c,PFT}} \quad (6)$$

Then crown bulk density was totaled across the number of cohorts for each PFT ($N_c PFT$) and summed across tree PFTs to get canopy bulk density (*CBD*) at each layer in the canopy:

$$CBD_l = \sum_{PFT=1}^{6} \sum_{c=1}^{N_c PFT} cbd_{l,c,PFT} \quad (7)$$

Canopy base height was determined as the layer height at which the summed canopy bulk density for all PFT cohorts was above the minimum threshold of 0.012 (kg m^{-3}) (Reinhardt et al., 2006). Canopy height was determined as the height at which the summed canopy bulk density for all PFTs dropped below the minimum threshold (Reinhardt et al., 2006). The canopy base height was then used as the critical scorch height for crown fire initiation. Thereby, in following with Van Wagner's theory (1977), when surface fire intensity reaches the critical value for scorch height to exceed canopy base height (*CBH*), crown fire is considered initiated in LMfireCF:

$$CFI = \begin{cases} 1, & SH > CBH \\ 0, & SH \le CBH \end{cases} \quad (8)$$

Two criteria defined critical conditions for crown fire spread: average canopy bulk density above a minimum threshold (0.10 kg m^{-3}) (Reinhardt et al., 2006) and canopy foliar moisture content equal to or below a maximum threshold (80%). These thresholds were calibrated to yield active crown fire in LMfireCF while being consistent with values in the literature. The average canopy bulk density (CBD_{avg}) was calculated by averaging each layer (*l*) from canopy base height (*CBH*) to canopy height (*CH*),

$$CBD_{avg} = \frac{\sum_{l=CBH}^{CH} CBD_l}{CH - CBH} \quad (9)$$

and the average canopy bulk density is assumed to be uniform throughout its depth (Keane et al., 1998).

Canopy foliar moisture content was assumed to be within the range of 50–150% (Scott and Reinhardt, 2001; Van Wagner, 1977). The daily water stress (water scalar; ratio of effective water supply to demand) for each tree PFT was weighted by its foliar projective cover relative to total tree cover to calculate mean daily canopy foliar moisture content in LPJ-GUESS-LMfireCF. If both conditions are met; average canopy bulk density (CBD_{avg}) and canopy foliar moisture (*cfm*) are above their respective thresholds, then crown fire will spread:

$$CFS = \begin{cases} 1, & if\ CBD_{avg} > 0.10\ and\ cfm \le 0.80 \\ 0, & otherwise \end{cases} \quad (10)$$

Eq. (4) can then be written as:

$$CF = \begin{cases} 1, & if\ SH > CBH\ and\ if\ CBD_{avg} > 0.10\ and\ cfm \le 0.80 \\ 0, & otherwise \end{cases} \quad (11)$$

In LPJ-GUESS-LMfireCF if the critical conditions were met for both crown fire initiation and crown fire spread, then active crown fire is assumed to occur, killing 100% of trees in the patch (Scott and Reinhardt, 2001). If these conditions are not met, mortality can still occur due to crown kill for a given PFT cohort, proportional to the ratio of the tree height to the scorch height (Pfeiffer et al., 2013), which may be considered a representation of passive crown fire. Importantly, mortality due to crown kill operates on individual PFT cohorts in LPJ-GUESS-LMfireCF as opposed to the average individual (PFT population) in a patch in LPJ-LMfire, allowing taller PFT cohorts to survive within a patch from passive crown fires.

2.8. Driver data

Daymet version 3 and TopoWx version 1.3.0 gridded daily climate data from 1980 to 2016 were used as input for LPJ-GUESS-LMfireCF (Oyler et al., 2015; Thornton et al., 2017). Mean monthly instantaneous downward shortwave radiation for 24 h was calculated from Daymet daily daylight average incident shortwave radiation. Total monthly precipitation was summed from Daymet daily precipitation, and the number of days in a month with precipitation summed to create monthly wet days. Mean monthly mean, minimum, and maximum air temperature was calculated from daily minimum and maximum air temperature for TopoWx1.3.0. The Modern-Era Retrospective analysis for Research and Applications, Version 2 (MERRA-2, (Gelaro et al., 2017)) monthly eastward wind speed of lowest model layer and northward wind speed of lowest model layer were used to calculate the horizontal wind speed vector using the Pythagorean Theorem, then resampled using R package 'raster' from ~50 km to 1km-resolution (Hijmans, 2019). Mean monthly lightning strike values were calculated from World Wide Lightning Location Network data (Lay, 2004). Due to the increase in sensors through space and time, the mean monthly value across the GYE for 2010–2014 was used for all pixels. Annual global atmospheric carbon dioxide concentrations from 1860 to 2016

(Le Quéré et al., 2018) were used for all GYE pixels. The multilayer soil characteristic gridded data for the conterminous United States (CONUS-Soil) based on the USDA State Soil Geographic Database (Miller and White, 1998) was infilled with Harmonized World Soil Database v. 1.2 for areas with missing data (Fischer et al., 2008) to provide continuous soil data for the region. Since LPJ-GUESS version 2.0 used in this study does not include soil nutrient limitations, a binary soil layer (Appendix D, Figure D1) indicating whether a grid cell had inceptisol soils or not was created from YNP soil type data (Rodman et al., 1996). Processing of model driver data was completed using Climate Data Operators (Schulzweida, 2019), NCO netCDF Operators (Zender, 2014), and R packages: raster (Hijmans, 2019), rgdal (Bivand et al., 2018), and ncdf4 (Pierce, 2017).

2.9. Model evaluation datasets

The performance of LPJ-GUESS-LMfireCF was evaluated in four areas: biomass, dominant plant cover, fire activity, and forest regeneration. Estimates of carbon in aboveground live vegetation from the USDA Forest Service's FIA field measurements (Gillespie, 1999) of 312 plots in YNP measured between 1999 and 2009, were used to benchmark simulated live aboveground carbon in vegetation. Estimates of aboveground live biomass for the year 2010 from the European Space Agency's satellite-based GlobBiomass project (Santoro, 2018) were used to benchmark simulated live carbon in vegetation for all of YNP. GlobBiomass live aboveground biomass estimates were multiplied by 0.5 to approximate carbon in live vegetation, assuming carbon content of biomass is about 50% (Penman et al., 2003). It is important to note that GlobBiomass estimations of carbon in vegetation are only aboveground, while values simulated in LPJ-GUESS include belowground carbon in the roots, which could account for about 20–30% (Cairns et al., 1997; Litton et al., 2003; Santantonio et al., 1977). To account for this difference, simulated carbon in vegetation was multiplied by 0.8 to approximate carbon in aboveground live vegetation to compare to GlobBiomass and FIA data. Simulated PFT distributions and cover were compared to the National Park Service's Yellowstone 1999 Cover Type data, a geodatabase of habitat type and land cover layers created from aerial photography and field surveys (Despain, 1990). Simulated fire area burned, fire severity, and fire frequency were compared to Monitoring Trends in Burned Severity (MTBS) data from 1984 to 2016 ("MTBS Data Access: Fire Level Geospatial Data," 2017) and fire perimeter data acquired from the Yellowstone National Park Spatial Analysis Center (provided by Alex Zaideman). Field data of forest carbon storage and leaf area index in lodgepole pine dominated sites in YNP were used to evaluate simulated postfire recovery with sites that burned in the 1988 Yellowstone fires sampled 11 and 24 years postfire to measure forest recovery (Turner et al., 2017, 2016, 2004) and for mature lodgepole pine forests (>100 years old) from a 300 year chronosequence (Kashian et al., 2013, 2012).

2.10. Statistical analysis

Normalized mean square error (NMSE) was used to quantify the range of spatial correlation between simulated total live aboveground carbon and GlobBiomass estimates, because it is less sensitive to extreme values than using the standard deviation and it does not require uncertainty estimates which are unavailable for simulation results (Kelley et al., 2013). NMSE was calculated as:

$$NMSE = \sum_i (y_i - x_i)^2 \Big/ \sum_i \left(y_i - \bar{x}_i\right)^2 \quad (12)$$

where, y_i is the modeled value in grid cell i, x_i is the corresponding value in the benchmarking dataset, and $\bar{x}_i$ is the mean value across all grid cells in the benchmarking dataset (Kelley et al., 2013). A NMSE value of zero indicates perfect agreement, values >1 suggest the model's performance is worse than the null model, and more generally smaller values denote better model performance. Welch two sample t-tests were used to compare biomass and LAI for regenerating and mature lodgepole pine forests between simulation results and field estimates (RStudio Team, 2016). The Welch's test was used because it does not assume equal variance. To lessen the spatial autocorrelation in the simulated data, 300 points were randomly selected from the 14,000+ grid cells simulated and statistical tests were performed on this smaller sample (Dale and Fortin, 2002).

3. Results

3.1. Landscape biomass

Fire model development in combination with the newly parameterized regional PFTs greatly improved modeled live carbon in vegetation relative to LPJ-GUESS-GlobFIRM (Fig. 5). Field data from FIA plots estimated mean total live aboveground carbon to be 50.8 ± 2.04 Mg C ha^{-1} (range 0–201 Mg C ha^{-1}), with measurements limited to forested areas. Estimates from field data were higher than the satellite-based GlobBiomass estimates and LPJ-GUESS-LMfireCF simulation results, which included non-forested grid cells. GlobBiomass, a spatially continuous dataset was our best reference for total YNP biomass estimates, with estimated mean live aboveground carbon in vegetation at 27.7 Mg C ha^{-1} with a total of 39.9 Tg C for the entire YNP for the year 2010 (Table 3). Simulated carbon in vegetation using LPJ-GUESS-LMfireCF with regional PFTs for 2010 resulted in a mean live aboveground carbon in vegetation of 31 Mg C ha^{-1} with a total of 44.8 Tg C for YNP, a 12% overestimation compared to GlobBiomass benchmark data. In comparison, simulated carbon in vegetation using LPJ-GUESS with the GlobFIRM fire module and global PFTs resulted in mean carbon in vegetation of 156 Mg C ha^{-1} with a total of 225 Tg C for YNP, five times the GlobBiomass estimated carbon in vegetation for YNP. The simulation using GlobFIRM with the regional PFTs resulted in mean carbon in

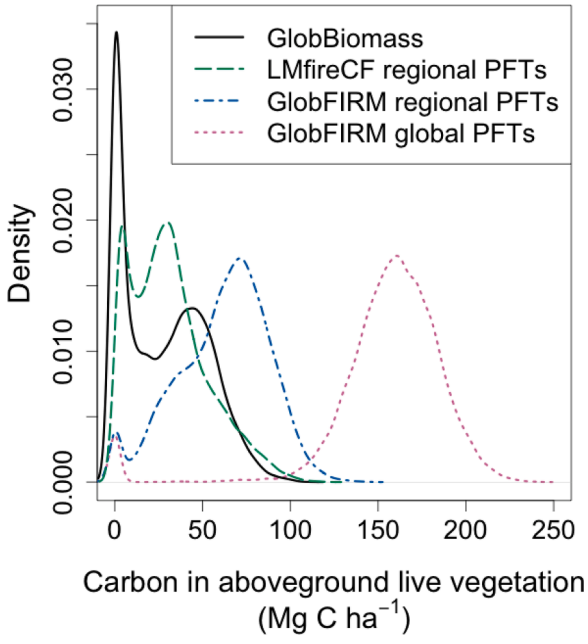

Fig. 5. Density curves for carbon in aboveground live vegetation (Mg C ha^{-1}) within Yellowstone National Park for year 2010 from the European Space Agency's satellite-based GlobBiomass estimates (solid line) and simulated by LPJ-GUESS (dashed lines) with either the LMfireCF fire module with regional plant functional types (PFTs, green dashed line), the GlobFIRM fire model with regional PFTs (blue dot-dashed line), or the GlobFIRM fire model with Global PFTs (purple dotted line). (For interpretation of the references to colour in this figure legend, the reader is referred to the web version of this article.)

vegetation of 61.7 Mg C ha^{-1} with a total of 89 Tg C for YNP, double the GlobBiomass estimates. In summary, the newly developed LPJ-GUESS-LMfireCF with regional PFTs showed a 97% reduction in simulated biomass estimate error compared to LPJ-GUESS-GlobFIRM with global PFTs.

Mapped distributions of LPJ-GUESS-LMfireCF simulated and GlobBiomass estimated carbon in vegetation are shown in Fig. 6a-b. Estimates of carbon in vegetation in the areas dominated by lodgepole pine are comparable between simulated and GlobBiomass estimates. However, carbon in vegetation at higher elevation areas in YNP, simulated as dominated by spruce-fir (Fig. 7), are overestimated compared to GlobBiomass (Fig. 6c). The areas of underestimated biomass in the western and southern edges of YNP (Fig. 6c) correspond with areas that were simulated as grass dominated that are actually forested (Fig. 7), but where uncertainty (reported as standard error) was higher for GlobBiomass (Fig. 6d). Normalized mean square error (NMSE) values indicate that model performance was greatly improved by using the LMfireCF fire module and regional PFTs, but all simulation results performed worse than the null model in estimating aboveground carbon (Table 3).

3.2. Dominant plant cover

For the new carbon allocation scheme, the size-dependent leaf area to sapwood area ratio resulted in more reasonable tree heights. Linear relationships between tree height and crown length showed a strong

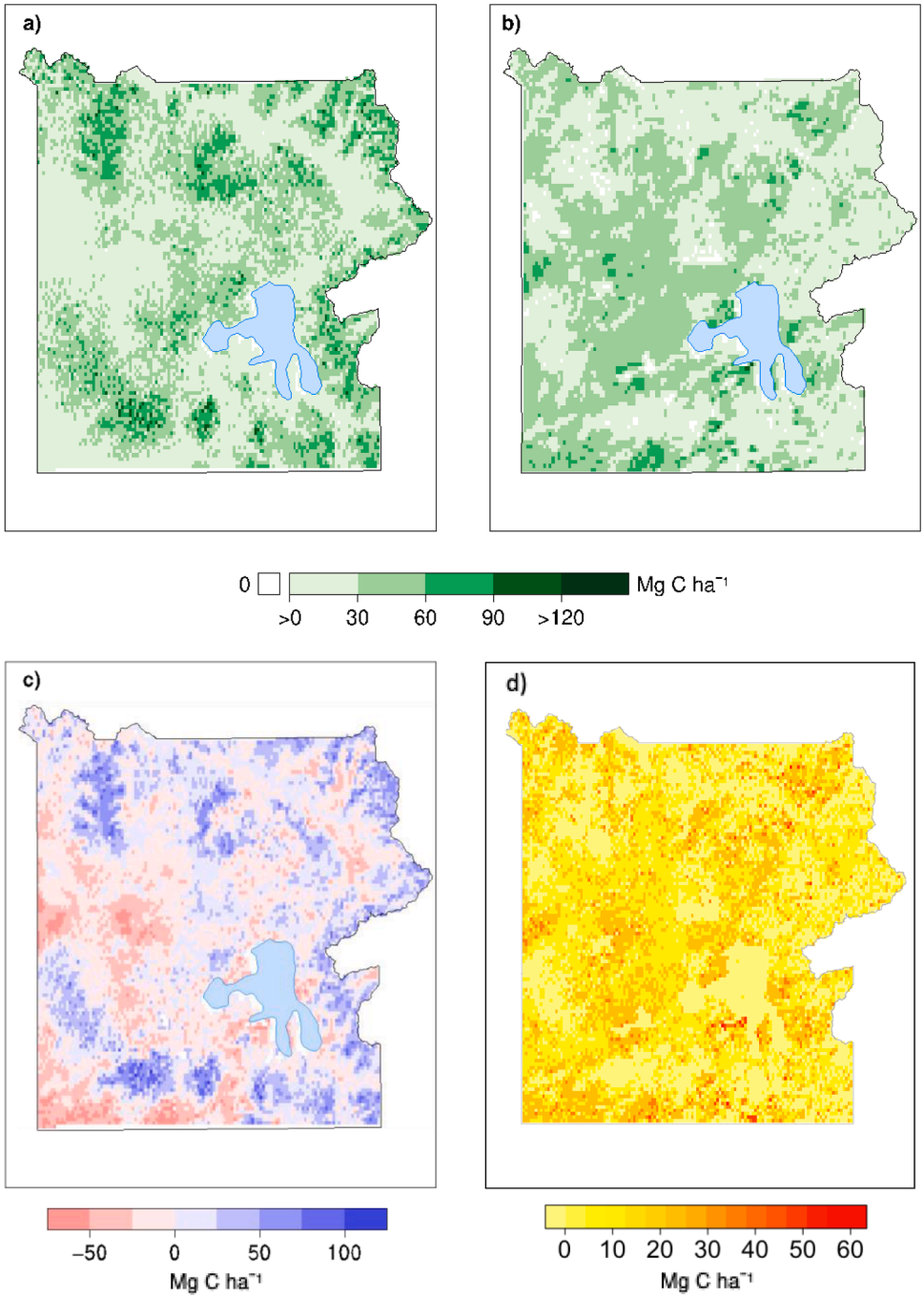

Fig. 6. Carbon in aboveground live vegetation (Mg C ha^{-1}) within Yellowstone National Park for 2010 a) simulated by LPJ-GUESS-LMfireCF b) European Space Agency's satellite-based GlobBiomass estimates, and c) difference between simulated, GlobBiomass estimates, and d) GlobBiomass uncertainty as standard error.

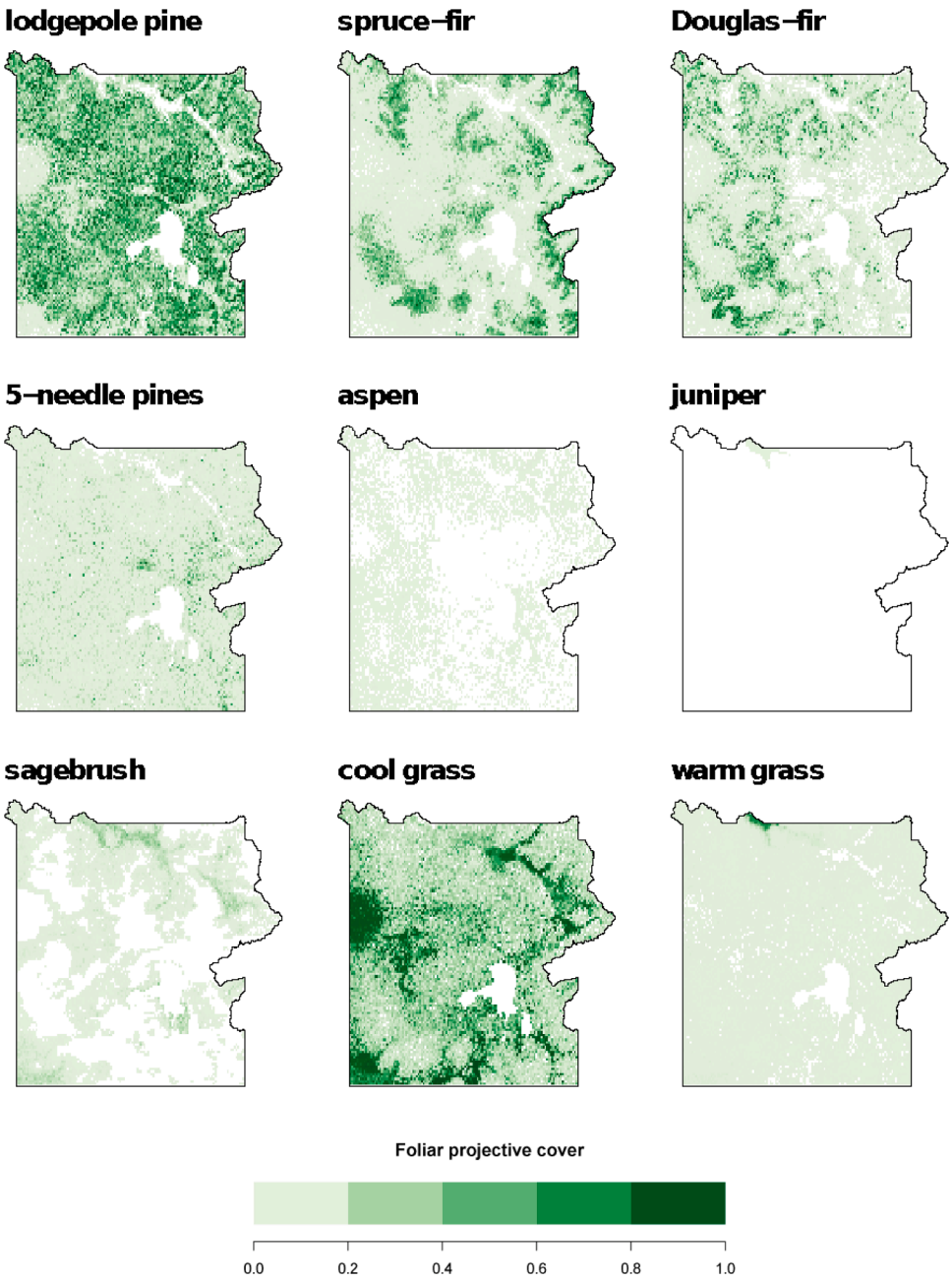

Fig. 7. LPJ-GUESS-LMfireCF simulated foliar projective cover under full leaf cover as fraction of modeled area averaged from 1997 to 2016 for regional plant functional types: lodgepole pine (*Pinus contorta*), a spruce-fir (*Picea engelmannii* and *Abies lasiocarpa*), Douglas-fir (*Pseudotsuga menziesii*), 5-needle pines (*Pinus albicaulis* and *Pinus flexilis*), aspen (*Populus tremuloides),* juniper (*Juniperus scopulorum*), sagebrush (*Artemisia tridentata*), a multi-species cool grass (C_3, for the photosynthetic pathway), and a multi-species warm grass (C_4).

correlation for all conifers (R^2 ranged from 0.51 to 0.97) and a moderate correlation for the deciduous PFT ($R^2 = 0.34$) (Appendix B). The linear regression equations better fit the data than the quadratic regression equations, so the linear slope and intercept values were used to calculate variable crown length based on height in LPJ-GUESS-LMfireCF by PFT.

To evaluate the ability of LPJ-GUESS-LMfireCF to simulate dominant plant foliar projective cover, the fraction of modeled area covered when under full leaf cover was mapped for each PFT across YNP. Simulated PFT foliar projective cover (Fig. 7) corresponded well with mapped National Park Service's (NPS) Yellowstone primary cover types from 1999 (Fig. 4). The simulated distribution of lodgepole pine matched well with the NPS distribution, with lodgepole pine dominating the largest area of Yellowstone. Simulated spruce-fir (Engelmann spruce and subalpine fir) occurrence in higher elevation regions of the park is accurate, but extensive areas are actually dominated by whitebark pine in the observational data. Douglas-fir, quaking aspen, and sagebrush cover was highest at lower elevations. The nonforested areas in the northern region of the park (Lamar Valley, Fig. 4) were simulated as grass dominated.

LPJ-GUESS-GlobFIRM simulated PFT foliar projective cover (Appendix E, Figure E1) resulted in spruce-fir dominating the largest area of Yellowstone. In comparison to LPJ-GUESS-LMfireCF results, the range of area dominated by other PFTs were contracted in the LPJ-GUESS-GlobFIRM simulation. Lodgepole pine, Douglas-fir, and cool grasses had greatly reduced cover using the GlobFIRM fire module. In the GlobFIRM simulation, spruce-fir dominated areas that LMfireCF simulated as lodgepole pine or Douglas-fir dominant. GlobFIRM simulated lodgepole pine dominated areas that LMfireCF simulated as cool grasslands.

3.3. Fire activity

LPJ-GUESS-LMfireCF fire activity, evaluated on total area burned and burn severity, was greatly improved with our modifications. Total area burned from 1984 to 2016 from MTBS data shows that 1988 and

2016 were the largest fire years in the record (Fig. 8). LPJ-GUESS-LMfireCF simulated 1988 as the largest fire year and 2016 as a large fire year, but also simulated notable area burned in 1994, 2000, 2003, 2008, and 2012. LPJ-GUESS-LMfireCF simulated that 25% of the area of YNP burned in 1988. MTBS and Yellowstone National Park Spatial Analysis Center fire mapping show that about 36% of the area of YNP burned in the1988 Yellowstone Fires.

In terms of fire severity, the predominant fire regime in YNP is characterized by stand-replacing crown fires. To compare the fire modules, a time series of live and dead combusted carbon and unconsumed carbon of fire-killed trees was plotted from 1984 to 2016 (Fig. 9). While GlobFIRM simulated 1988 as a fire year, fire severity was low throughout the simulation period. In contrast, LMfireCF simulated 1988 more accurately as a high severity fire year, with affected carbon in vegetation proportional to area burned. Although LMFireCF showed a large spike in affected carbon in vegetation in 1988, ~70% of the carbon remained in the system as litter. The discrepancy in fire severity between LMfireCF and GlobFIRM is shown in Fig. 10, with LMfireCF causing a ~28% reduction in aboveground carbon in live vegetation across YNP from the 1988 fires, compared to insignificant perturbations in carbon due to fire for GlobFIRM throughout the simulation period (Fig. 10).

3.4. Forest regeneration

Lodgepole pine stands regenerated quickly after the 1988 fires in YNP, both in field measurements and LPJ-GUESS-LMfireCF simulations (Table 4). From the simulated burned area in 1988, grid cells were subset that were previously dominated by lodgepole pine (>50% foliar projective cover), extensively burned (>80% fraction burned), and did not burn again on or before 24 years postfire. For these subset grid cells, LPJ-GUESS-LMfireCF (n = 240) simulated mean live aboveground biomass (25.7±1.16 Mg ha^{-1}) was seven times greater than field estimations 11 years postfire (3.38±0.65 Mg ha^{-1}) and the range was twice the field estimate (Table 4). In postfire year 24, simulated mean live biomass (40.1±1.65 Mg ha^{-1}) was 58% greater than field estimations (25.4±2.5 Mg ha^{-1}), but with a similar range. Simulated leaf area index (LAI) was more than two times greater than field estimations, 11 and 24 years postfire (Table 4). The time series of aboveground carbon in live vegetation LPJ-GUESS-LMfireCF simulated across YNP (Fig. 10) shows a gradual recovery, with declines corresponding with fire activity. Comparing biomass for mature lodgepole pine forests, field-based estimates (76.6±3.5 Mg ha^{-1}) were greater than simulation results for both model configurations (Table 4). Interestingly, the Welch two sample t-test indicated no evidence of a true difference in mean between simulated results and field estimates for LAI in mature forests (p>0.01), indicating potential model bias in carbon allocation to sapwood carbon pools over leaf carbon pools.

For a subset of grid cells, LPJ-GUESS-GlobFIRM (n = 152) was a much poorer predictor, with simulated mean live biomass (54.3±1.8 Mg ha^{-1}) sixteen times greater than field estimations 11 years postfire, with almost four times the range (Table 4). In postfire year 24, LPJ-GUESS-GlobFIRM simulated biomass had declined, but the mean remained 94% greater than the field estimated. Based on observations biomass should continue to increase for about 90–100 years post fire (Kashian et al., 2013). LPJ-GUESS-GlobFIRM simulated mean LAI was more than three times greater than field estimated 11 years postfire and because simulated LAI declined, was closer to field estimated 24 years postfire, but still overestimated. These subset grid cells burned in 1988 and did not reburn, so declines in biomass and LAI were due to other forms of mortality represented in the model (e.g. longevity, carbon limitation). The low severity fires simulated by LPJ-GUESS-GlobFIRM resulted in carbon in vegetation fluctuations due to fire being minor perturbations (Fig. 10).

4. Discussion

4.1. Landscape biomass

Developments included in LPJ-GUESS-LMfireCF improved model performance in simulating carbon in vegetation in YNP compared to LPJ-GUESS with the GlobFIRM fire module (Fig. 5). The parameterization of regional PFTs (blue dash-dot line) compared to global PFTs (purple dotted line) also improved model performance in simulating carbon. Total carbon in vegetation in YNP was overestimated by 12% by LPJ-GUESS-LMfireCF with regional PFTs (green dashed line) compared to GlobBiomass estimations (solid black line), a 97% reduction in simulated biomass estimate error compared to LPJ-GUESS-GlobFIRM with global PFTs. This demonstrates that both the newly parameterized regional PFTs and the process-based model developments individually and combined resulted in more accurate representation of reality. Individual grid cell diagnostic plots (Appendix F: Figure F1 and F2) suggest the newly developed crown fire dynamics routine specifically was a critical process-based model development. When the crown fire module was disabled (LMfire), fires occurred at lower severity and more frequently from 1980 to 2016 than when using LMfireCF (Figure F1). Using LMfire aboveground carbon in live vegetation continued to accumulate until the late 1990's when it gradually declined (Figure F2), indicative of PFT longevity-based mortality in LPJ-GUESS for an individual grid cell. In contrast, using LMfireCF maximum aboveground carbon in live vegetation is about half of the maximum using LMfire during the timeseries (Fig. F2).

The remaining discrepancy in simulated carbon in vegetation compared to satellite-based estimates is the long-tailed distribution simulated by LPJ-GUESS-LMfireCF (Fig. 5), which is due to the overestimation of carbon in vegetation at higher elevation areas in YNP (Fig. 6c). In our simulations, these areas with over-estimated biomass corresponded with areas dominated by the spruce-fir PFT (Engelmann spruce and subalpine fir, Fig. 7). Adjusting parameters for the spruce-fir

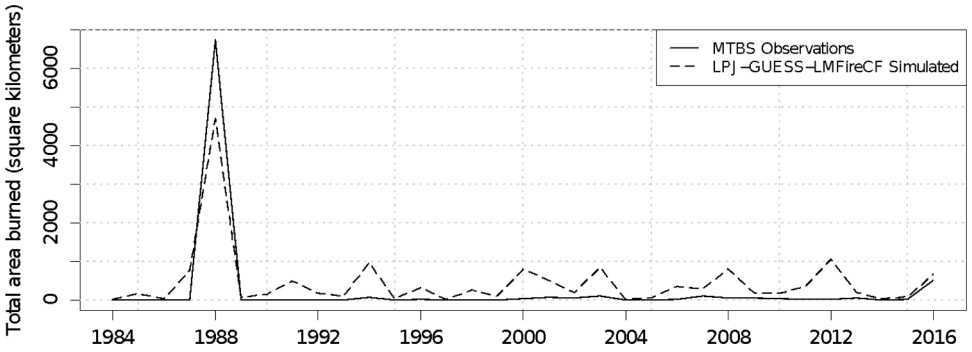

Fig. 8. Time series of total area burned in square kilometers from 1984 to 2016 within Yellowstone National Park showing Monitoring Trends in Burned Severity (MTBS) observations (solid line) and simulated by LPJ-GUESS-LMfireCF (dashed line).

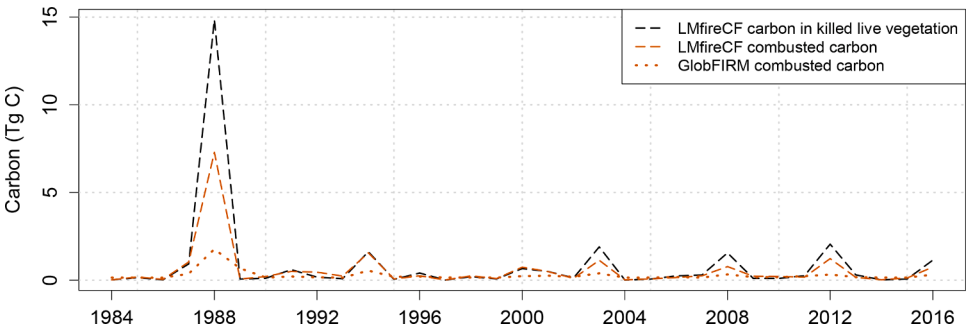

Fig. 9. Carbon (Tg C) from combustion of live and dead vegetation (red lines) and unconsumed carbon (Tg C) of trees killed by fire and transferred to litter (black line) from 1984 to 2016 within Yellowstone National Park simulated by LPJ-GUESS using GlobFIRM (dotted line) and LMfireCF (dashed line) fire modules, both using regional plant functional types. In LMfireCF combusted carbon that is emitted to the atmosphere, is distinguished from carbon in killed live vegetation that is transferred to litter. In GlobFIRM live vegetation killed by fire is emitted to the atmosphere. (For interpretation of the references to colour in this figure legend, the reader is referred to the web version of this article.)

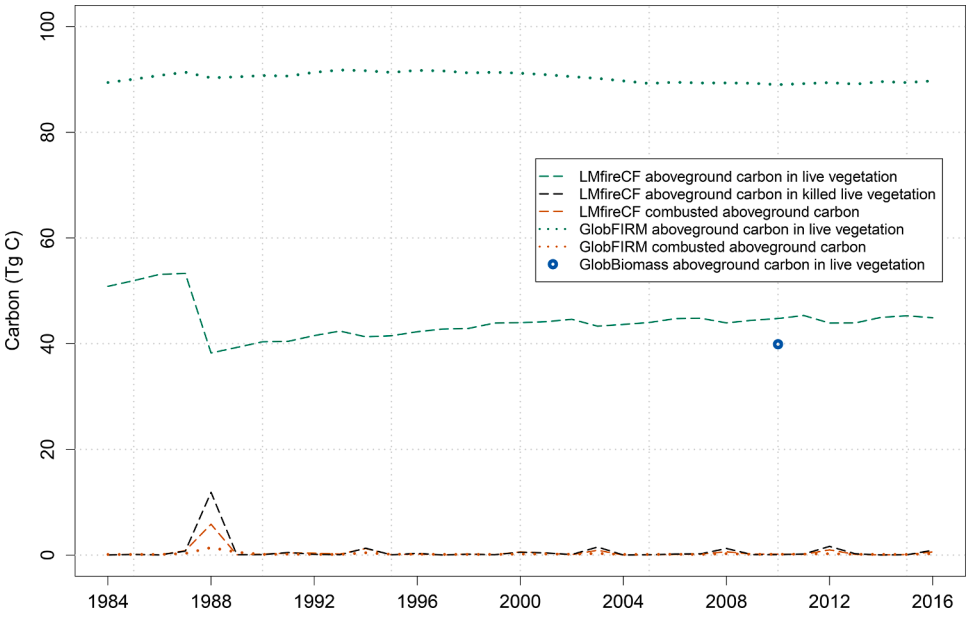

Fig. 10. Time series of aboveground carbon in live vegetation (green lines), combusted aboveground carbon (red lines), and aboveground carbon in killed live vegetation (black line) in metric tons of carbon (Tg C) from 1984 to 2016 within Yellowstone National Park simulated by LPJ-GUESS using GlobFIRM (dotted lines) and LMfireCF (dashed lines) fire modules, both using regional plant functional types. In LMfireCF combusted carbon that is emitted to the atmosphere, is distinguished from carbon in killed live vegetation that is transferred to litter. In GlobFIRM live vegetation killed by fire is emitted to the atmosphere. European Space Agency's satellite-based GlobBiomass 2010 estimate (point) of carbon in aboveground live vegetation. (For interpretation of the references to colour in this figure legend, the reader is referred to the web version of this article.)

PFT could reduce its dominance and carbon accumulation, improving modeled estimates of carbon in YNP. Yet, much of this area extent in YNP is occupied by whitebark pine in the NPS's cover type data (Fig. 4). However, whitebark pine communities have suffered extensive mortality in the Yellowstone region due to mountain pine beetle (*Dendroctonus ponderosae*) outbreaks and white pine blister rust (*Cronartium ribicola*) infections (Shanahan et al., 2016). Much of the higher elevation areas labeled as "non-vegetated" in the satellite-based GlobBiomass dataset could be areas of whitebark pine die-off. Even if the high elevation pines PFT were simulated to occupy these areas, mortality due to bark beetle outbreaks and white pine blister rust would not be captured. Disturbance agents other than fire are not explicitly modeled in LPJ-GUESS v. 2.0, instead a generic patch disturbance can be enabled that randomly kills patches at a user defined time interval (e.g. 100 years). Further model development is needed for these pest and pathogen disturbance dynamics to be represented for the GYE, although there were efforts to simulate impacts of European spruce bark beetle (*Ips typographus*) outbreaks in Sweden (Jönsson et al., 2012).

Underestimated biomass in the western side and southwest corner of YNP correspond with areas simulated as dominated by the C_3, cool grass PFT. The distribution of the cool grass PFT strongly matches climatological mean distributions of mean temperature and annual precipitation. These areas are lodgepole pine dominated in the NPS's Yellowstone cover type data, implying that the bioclimatic limits of the lodgepole pine PFT may need to be adjusted to allow more growth in these areas.

4.2. Dominant plant cover

Simulating regional PFTs was critical to approaching satellite-based estimates of distribution of biomass in the landscape. Global PFTs were so generalized that one PFT type (boreal needleleaved evergreen, see Table 2) dominated the landscape. This implies that for regional scale resolution, DGVM simulations must include more PFTs to be representative of the vegetation dynamics. While lodgepole pine dominates YNP, there still remain important vegetation patterns with elevation that are not captured with only one productive PFT. The newly parameterized PFTs recreated distinct vegetation types with elevation. Lower-elevations were dominated by grass, sagebrush, and Douglas-fir, typical of the region. The subalpine was dominated predominately by lodgepole pine with some co-occurrence of Douglas-fir at lower elevations and Engelmann spruce and subalpine fir (CW con) at higher elevations.

The simulated dominance of lodgepole pine in YNP on non-rhyolitic soils was dependent on the fire module simulating high severity crown fires. Lodgepole pine is a relatively fast growing species and in the absence of fire, more shade tolerant and slower growing species will grow in the understory and then dominate the subalpine overstory (Romme, 1982). However, on rhyolitic soils this transition of dominant species does not occur and lodgepole continues to dominate (Despain, 1983). In the case of YNP on non-rhyolitic soils, these more shade tolerant species or climax species are Engelmann spruce, subalpine fir,

Table 2
Global plant functional types (PFTs) used for LPJ-GUESS simulations with three descriptive model parameters (Smith et al., 2001). BNE = boreal needleleaved evergreen, BINE = boreal shade-intolerant needleaved evergreen, BNS = boreal needleleaved summergreen, TeBS = temperate broadleaved summergreen, IBS = shade-intolerant broadleaved summergreen, TeBE = temperate broadleaved evergreen, TrBE = tropical broadleaved evergreen, TrIBE = tropical shade-intolerant broadleaved evergreen, TrBR = tropical broadleaved raingreen, and C_3 = cool grass (C_3 photosynthetic pathway), and C_4 = warm grass (C_4 photosynthetic pathway). Geographic ranges correspond with different optimum temperatures for photosynthesis.

Description & Parameters	PFT BNE	BINE	BNS	TeBS	IBS	TeBE	TrBE	TrIBE	TrBR	C3	C4
Geographic range	boreal	boreal	boreal	temperate	boreal	temperate	tropical	tropical	tropical	*NA*	*NA*
Growth form	tree	tree	tree	tree	tree	tree	tree	tree	shrub	grass	grass
Phenology	evergreen	evergreen	summergreen (SG)	SG	SG	evergreen	evergreen	evergreen	raingreen	SG	SG
Shade tolerance class	tolerant	intolerant	intolerant	tolerant	intolerant	tolerant	tolerant	intolerant	intolerant	*NA*	*NA*

Table 3
Total live aboveground carbon estimates from satellite-based GlobBiomass and simulated by LPJ-GUESS with regional plant functional types using either LMfireCF or GlobFIRM fire module for all elevation zones in Yellowstone National Park. The normalized mean square error was calculated to quantify the range of spatial correlation between simulated total live aboveground carbon and GlobBiomass estimates.

Total live aboveground carbon	All Elevation Zones (MgC ha^{-1}) Mean	Min-Max	NMSE	Total YNP (TgC)	% Difference
GlobBiomass^	27.7±0.19	0–109	1	39.9	
LPJ-GUESS-LMfireCF+ (regional PFTs)	31.0±0.18	0–120	1.95	44.8	12
LPJ-GUESS-GlobFIRM+ (regional PFTs)	61.7±0.2	0–145	4.14	89	223
LPJ-GUESS-GlobFIRM+ (global PFTs)	156±0.2	0–240	31.7	225	563

Notes: Error measurement is standard error.
^ GlobBiomass estimates are from 2010. NMSE is reported for comparison with the mean model.
+ LPJ-GUESS YNP estimates are from simulated year 2010.

and, at the higher elevations, whitebark pine (Romme, 1982) simulated as two PFTs: spruce-fir and 5-needle pines. The co-occurrence and dominance of the spruce-fir PFT in higher elevations is due to lower simulated fire activity and the absence of inceptisol soils, allowing them to outcompete lodgepole pine PFT. The fire module GlobFIRM failed to capture high-severity fires, so the spruce-fir PFT dominated a larger portion of YNP compared to the LMfireCF module.

However, the dominance of whitebark pine in the highest regions of the park was missing in the distribution of the high-elevation 5-needle pines PFT (whitebark and limber pine), regardless of the fire module applied. These two distinct pine species were combined into one PFT due to the lack of complete knowledge of their unique bioclimatic limits and other physiological characteristics (Weaver, 2001) needed for parameterization. The actual distributions of whitebark and limber pines sometimes overlap (Arno and Hoff, 1989; McCaughey and Schmidt, 1990), and in the field the species can only be distinguished by their female cones, and less reliably by their male cones (Weaver, 2001). The tendency of whitebark pine to grow at higher elevations than limber pine led to the adoption of an elevation threshold "rule of thumb" used for vegetation simulations (Clark et al., 2017). Even in paleoecological reconstructions of regional vegetation, whitebark and limber pine distributions are indistinguishable because their pollen cannot be discriminated (Iglesias et al., 2015). Current research into distinguishing bioclimatic limits between whitebark and limber pine are underway (Hansen et al., 2016) and could lead to separate parameterization in LPJ-GUESS-LMfireCF simulations.

The importance of representing different vegetation zones became more apparent when we consider applying LPJ-GUESS-LMfireCF to simulate potential changes under projected future climate scenarios. In YNP there is concern over the potential contraction of forested vegetation types and expansion of sagebrush steppe/grassland vegetation types, as climate becomes more or less favorable to different vegetation types (Hansen and Phillips, 2015; Piekielek et al., 2016; Westerling et al., 2011). Such a vegetation type conversion would drastically reduce the amount of terrestrial stored carbon in YNP (Kashian et al., 2006). The ability of LPJ-GUESS to simulate multiple PFTs with different age-based cohorts within each grid cell allows it to simulate successional dynamics and vegetation zones (Hickler et al., 2012, 2004). Furthermore, since vegetation zones were emergent, not prescribed through initialization, they demonstrate prognostic capabilities of LPJ-GUESS-LMfireCF.

Table 4
Lodgepole pine leaf area index (LAI) and biomass: estimations from field data (Kashian et al., 2013; Turner et al., 2016) and simulated by LPJ-GUESS with regional plant functional types using either the LMfireCF or GlobFIRM fire module for postfire lodgepole pine stands regenerating 11 and 24 years after 1988 fires and for unburned mature forests (>100 years old) in Yellowstone National Park.

Lodgepole pine LAI and biomass	Postfire year 11 Mean	Median	Min-Max	Postfire year 24 Mean	Median	Min-Max	Mature Forests Mean	Median	Min-Max
Total live aboveground biomass (Mg ha^{-1})									
field estimations^	3.38±0.65	1.07	0–31.4	25.4±2.5	22.4	0–85.9	76.6±3.5	73.5	13.2–124.7
LPJ-GUESS-LMfireCF	25.7±1.16	26.9	0–62.9	40.1±1.65	44.0	0–81.4	58.4±0.8	56.8	33.9–115
LPJ-GUESS-GlobFIRM	54.3 ± 1.8	53.2	6.0–130	49.2 ± 1.89	47.1	3.32–148	66.6±1.3	62.9	30.4–239
Leaf area index (LAI) (m^2/m^2)									
field estimations^	0.74±0.14	0.21	0–6.7	1.16±0.11	1.03	0–4.0	2.84±0.12	2.8	1.16–5.39
LPJ-GUESS-LMfireCF+	2.03±0.07	2.13	0–4.42	2.65±0.86	2.97	0–4.74	3.13±0.03*	3.07	2.34–4.66
LPJ-GUESS-GlobFIRM+	2.31±0.06	2.31	0.19–4.06	2.05±0.06	2.08	0.04–4.05	3.1±0.03*	3.01	2.2–4.47

Notes: Error measurement is standard error.
^ Postfire estimates are from Turner et al. 2016 for 71 plots measured in 1999 and 2012. Mature forest estimates are from Kashian *et. al.* 2013 for 48 plots measured between 2004 and 2007.
+ Mature forest estimates are from simulation year 2016, randomly subset to $N = 300$.
* Welch two sample t-test $p > 0.01$, indicating no evidence of true difference in mean between simulated results and field estimates.

4.3. Fire activity

The model development represented here focused on capturing two key aspects of fire activity that are relevant to regional and global-scale fire modeling: burned area and fire severity. LPJ-GUESS-LMfireCF simulated large areas burned in 1988, 1994, 2000, 2003, 2008, 2012 and 2016. These were all years of notable fire activity in the larger GYE (Appendix F, Figure F1). These years correspond to years with low precipitation, indicating the sensitivity of the LMfireCF fire module to precipitation. Also, since LMfireCF does not simulate fire suppression, we expected to overestimate area burned. It may be that these simulated fire years could have become larger fire years in YNP in the absence of any fire suppression efforts or with increased lightning strikes.

The simulated area burned is the sum of area burned within each grid cell. In LMfireCF, the fraction burned of a grid cell is a function of fire rate of spread, slope, and wind speed (Pfeiffer et al., 2013). Fire rate of spread is dependent on the amount, density, and moisture of fuels, and wind speed. The representation of area burned as determined by modeled processes allows LMfireCF simulations to be responsive to changing conditions. In comparison, in GlobFIRM the fraction burned of a grid cell is based on an empirical relationship with fire season length (Thonicke et al., 2001, see Fig. 2). Utilizing fixed empirical relationships does not allow for the model to predict fire behavior under novel conditions. A more mechanistic fire module, like LMfireCF, can be more flexible to novel conditions.

However, LMfireCF has one important limitation; it does not model fire spread between grid cells and thereby cannot predict fire patterns or fire size. Since fire occurrence is emergent in LPJ-GUESS-LMfireCF as opposed to prescribed, there is no expectation that spatial patterns of fire would strongly correlate with observed fire patterns on the landscape. Moreover, it would be difficult to simulate the influence of past burned areas on restricting future fire spread. Under extreme weather conditions conducive to large fires, fire paths are most dictated by the current wind conditions (Bessie and Johnson, 1995). LMfireCF runs at a daily timestep so it does not capture the hourly fluctuations in weather conditions that drive the spread of large fires. Furthermore, as simulations in LPJ-GUESS are run as one grid cell at a time in sequence, as opposed to all grid cells at the same timestep in parallel, the model framework inhibits simulating the spread of fire between grid cells. Without cell-to-cell fire spread it is not possible to realistically simulate observed fire scars or fire extents, and to include the spatial interactions of fire pattern on future fire activity.

The greatest improvement to modeling fire behavior in YNP presented here was the simulation of high severity, stand-replacing crown fires from the development of crown fire dynamics in the LMfireCF fire module. In prior versions of LMfire, fire dynamics were based on the surface fire equations (Chaste et al., 2018; Pfeiffer et al., 2013). LMfire is most often used within LPJ which does not represent forest stand structure because it simulates average individuals of a PFT population. LPJ-GUESS simulates age-based PFT cohorts, simulating forest stand structure, enabling the distinction between surface and crown fires when coupled with a fire module that simulates both. The original fire module in LPJ-GUESS v. 2.0, GlobFIRM greatly underestimated fire severity in YNP simulations. Similarly, with the newly developed crown fire routine disabled, LPJ-GUESS-LMfire simulated low severity fires (Appendix F: Figures F1 and F2) unable to represent the high severity, stand-replacing crown fires characteristic of the region.

While in theory it would be possible to calibrate the parameters in these fire modules to simulate high severity fires in a given region, it diminishes the ability to also simulate mixed and low severity fires. Effectively, optimizing parameters in a surface fire module could compensate for the lack of crown fire dynamics, mimicking observations, i.e. equifinality (Tang and Zhuang, 2008), but would not be able to provide emergent results (Keane, 2019; Wilson and Botkin, 1990). By developing crown fire dynamics in LMfireCF, high severity fires were emergent based on complex interactions between vegetation, climate, and fire dynamics. LMfireCF is a fire module that is applicable to various fire regimes; surface or crown-fire dominated, as opposed to being over-calibrated to fit one fire regime.

Another important component of simulating fire severity is estimating carbon fluxes to the atmosphere due to fire. In GlobFIRM live aboveground biomass that is killed by fire and dead vegetation that is burned, is considered entirely combusted and added to the flux to the atmosphere that year (Smith et al., 2001; Thonicke et al., 2001). Both of these assumptions are incorrect. Even in stand replacing crown-fires the fine live and dead fuels may be combusted (1 and 10 hour fuels), but only a portion of larger live and dead fuels (100 and 1000 hour fuels) are combusted and instead remain in the ecosystem as deadwood. In LMfire and LMfireCF a fraction of live biomass killed is assumed to combust and the rest is transferred to litter (Chaste et al., 2018; Pfeiffer et al., 2013). It follows that if GlobFIRM is calibrated to simulate high-severity fires it would overestimate carbon fluxes to the atmosphere unless the module is altered. By LMfireCF partitioning live biomass killed by fire into combusted or added to litter it can estimate immediate (combustion) and delayed (decomposition or combustion in future fires) carbon fluxes to the atmosphere. Therefore, the distinction in LMfire of carbon that is combusted and carbon that is transferred to litter ensures that carbon fluxes and pools are more accurately simulated in LPJ-GUESS.

4.4. Forest regeneration

LPJ-GUESS-LMfireCF simulated more rapid lodgepole pine forest regeneration in YNP than estimated from field measurements. Further model developments could be implemented to improve results and these are described below. Post-fire lodgepole pine forest regeneration as measured by stem density varied with pre-fire serotiny levels, fire severity, and fire patch size (Turner et al., 1997). Serotiny was missing in LPJ-GUESS-LMfireCF, so all grid cells were assumed to have the same availability of propagules independent of their fire history, not including a critical restraint on lodgepole pine regeneration. More generally, PFT establishment was simulated as stochastic, with the number of saplings randomly drawn from a Poisson distribution constrained by a maximum sapling establishment rate (PFT specific parameter '*est_max*' (saplings/m^2/year)). Thereby variation in stem density between grid cells is based on bioclimatic limits to establishment and survival, and random probability. Yet, the *est_*max parameter value for lodgepole pine was set to one tenth the mean stem density 24 years after fire. Also, biomass was simulated as lower than field estimates for mature forests, implying growth curves need to be adjusted so growth rates are reduced for young cohorts. Growth rates are controlled by carbon assimilation, allocation, and allometry equations and associated parameters so these are the areas to focus further model development and calibration.

4.5. Future implications

Climate change is expected to alter the fire and vegetation dynamics in the YNP. Annual air temperature is expected to increase 1 to 5 °C in the GYE by 2099 (Chang and Hansen, 2015) . The climate conditions associated with large, high-severity fires are predicted to become common by mid to late century (Westerling et al., 2011). Warming and drying conditions that threaten seedling survival (Harvey et al., 2016) in conjunction with short-interval severe fires are projected to affect postfire subalpine forest regeneration (Hansen et al., 2018; Hansen and Turner, 2019; Turner et al., 2019). Suitable climate space for the dominant alpine and subalpine tree species is projected to decline, with expansion of suitable climate space for arid shrub and grasslands (Hansen and Phillips, 2015). All of these conditions combine to threaten the resiliency of subalpine forests in YNP and weaken carbon sinks (Turner et al., 2019).

Process-based models can help us address pressing questions about the impact of disturbance and climate interactions on forest regeneration and carbon storage in the future. Process-based forest simulation

models FireBGCv2 (Clark et al., 2017; Keane et al., 2011) and iLand (Hansen and Turner, 2019; Turner et al., 2019) have been applied to the YNP to make inferences about future dynamics. While both models predict decline of lodgepole pine dominated forest on the landscape, FireBGC predicts that forest cover will persist as Douglas-fir increases on the landscape (Clark et al., 2017) and iLand shows that Douglas-fir could also fail to regenerate under future climate scenarios (Hansen et al., 2018). The complexity and high-resolution of iLand and FireBGC limit the scale of simulations to individual stands up to watersheds. The advantage of LPJ-GUESS-LMfireCF is that by simulating age-based cohorts, instead of individual trees, the computational efficiency makes it possible to run simulations at regional up to global scales. The higher resolution forest simulation models appear to be better suited to address stand-level questions around mechanisms of regeneration failure. The strength of LPJ-GUESS-LMfireCF is that it can be applied to project regional level forest cover and carbon storage, while capturing landscape heterogeneity.

At the global scale, projections of the terrestrial carbon sink rely on predictions of forest biogeography, disturbance turnover, and forest regrowth. First, predictions of future vegetation cover rely on projections of human land use and land cover change (Arneth et al., 2017; Friedlingstein et al., 2019; Poulter et al., 2011), but also projections of future forest resiliency and species distributions (Walker et al., 2019; White et al., 2000). The use of regional PFTs in DGVMs as presented here can enhance the ability to model forest biogeography, simulating current vegetation zones along elevation and climate gradients. Using regional PFTs also improved simulated productivity, with biomass estimates drastically closer to benchmarking data than by using global PFTs. Secondly, even small changes in fire regimes could have a strong influence on the forest carbon sink (Pugh et al., 2019a). The influence of disturbance turnover on long-term carbon fluxes necessitates modeling of stand-replacing crown fire regimes (Pugh et al., 2019a). LPJ-GUESS-LMfireCF demonstrates the potential for modeling crown fire dynamics in DGVMs and the fire module described here may serve as precedent for developments in other DGVMs. Finally, forest regrowth may be responsible for more than half of the terrestrial carbon sink (Pugh et al., 2019a). DGVMs need to represent forest structure and successional dynamics to best estimate forest regrowth. LPJ-GUESS has been demonstrated to simulate forest structure and successional dynamics in several regional studies (Hickler et al., 2012, 2004; Smith et al., 2001), but further development of LPJ-GUESS-LMfireCF is needed to approximate estimates of biomass regrowth rates in regions with stand-replacing crown fire regimes.

Declaration of Competing Interest

The authors declare that they have no known competing financial interests or personal relationships that could have appeared to influence the work reported in this paper.

Acknowledgements

Thank you to Robert Keane, Monica Turner, Dave Roberts, and Andrew Hansen for their helpful feedback. Special thanks to Frances Ambrose for field data collection. Computations were performed on the Hyalite High Performance Computing System, operated and supported by University Information Technology Research Cyberinfrastructure at Montana State University; thank you to the staff administrators Pol Llovet, Erik Bryer, and Jonathan Hilmer, among others. KDE acknowledges funding from an NSF Graduate Research Fellowship Award No. DGE-1632134; and the Montana Institute on Ecosystems with support from NSF-IIA-1443108 and EPS-1101342; and a PhD Dissertation Completion Award from the Graduate School, Montana State University. The research was also supported, in part, by NSF Grant GSS-1461590 and Grant No. G15AP00073 from the United States Geological Survey. BP acknowledges support from NASA's Terrestrial Ecology Program. The authors would like to thank the World Wide Lightning Location Network (http://wwlln.net), a collaboration among over 50 universities and institutions, for providing the lightning location data used in this paper.

Supplementary materials

Supplementary material associated with this article can be found, in the online version, at doi:10.1016/j.ecolmodel.2020.109417.

References

Agee, J.K., 1996. Fire Ecology of Pacific Northwest Forests. Island Press.
Alexander, M.E., 1982. Calculating and interpreting forest fire intensities. Can. J. Bot. 60, 349–357. https://doi.org/10.1139/b82-048.
Arneth, A., Sitch, S., Pongratz, J., Stocker, B.D., Ciais, P., Poulter, B., Bayer, A.D., Bondeau, A., Calle, L., Chini, L.P., Gasser, T., Fader, M., Friedlingstein, P., Kato, E., Li, W., Lindeskog, M., Nabel, J.E.M.S., Pugh, T.A.M., Robertson, E., Viovy, N., Yue, C., Zaehle, S., 2017. Historical carbon dioxide emissions caused by land-use changes are possibly larger than assumed. Nat. Geosci 10, 79–84. https://doi.org/10.1038/ngeo2882.
Arno, S.F., Hoff, R.J., 1989. Silvics of Whitebark Pine (Pinus albicaulis) (No. INT-GTR-253). U.S. Department of Agriculture, Forest Service, Intermountain Research Station, Ogden, UT. https://doi.org/10.2737/INT-GTR-253.
Bachelet, D., Lenihan, J.M., Daly, C., Neilson, R.P., Ojima, D.S., Parton, W.J., 2001. MC1: A Dynamic Vegetation Model For Estimating the Distribution of Vegetation and Associated Ecosystem Fluxes of Carbon, Nutrients, and Water (General Technical Report), PNW-GTR-508. USDA Forest Service, Pacific Northwest Research Station.
Baker, William L., 2009. Lightning, Fuels, Topography, Climate, and Fire Behavior. Fire ecology in Rocky Mountain landscapes. Island Press, Washington D.C., p. 20
Barrett, S.W., 1994. Fire regimes on andesitic mountain Terrain in Northeastern Yellowstone National Park, Wyoming. Int. J. Wildland Fire 4, 65–76.
Bessie, W.C., Johnson, E.A., 1995. The relative importance of fuels and weather on fire behavior in subalpine forests. Ecology 76, 747–762. https://doi.org/10.2307/1939341.
Bivand, R., Keitt, T., Rowlingson, B., 2018. rgdal: Bindings for the "Geospatial". Data Abstraction Library.
Brown, J.K., Reinhardt, E.D., Fischer, W.C., 1991. Predicting Duff and Woody fuel consumption in northern idaho prescribed fires. For. Sci. 37, 1550–1566.
Cairns, M.A., Brown, S., Helmer, E.H., Baumgardner, G.A., 1997. Root biomass allocation in the world's upland forests. Oecologia 111, 1–11. https://doi.org/10.1007/s004420050201.
Chang, T., Hansen, A., 2015. Historic & projected climate change in the greater yellowstone ecosystem. Yellowstone Sci. 23, 14–19.
Chaste, E., Girardin, M.P., Kaplan, J.O., Portier, J., Bergeron, Y., Hély, C., 2018. The pyrogeography of eastern boreal Canada from 1901 to 2012 simulated with the LPJ-LMfire model. Biogeosciences 15, 1273–1292. https://doi.org/10.5194/bg-15-1273-2018.
Clark, J.A., Loehman, R.A., Keane, R.E., 2017. Climate changes and wildfire alter vegetation of Yellowstone National Park, but forest cover persists. Ecosphere 8, 1–16. https://doi.org/10.1002/ecs2.1636.
Cosby, B.J., Hornberger, G.M., Clapp, R.B., Ginn, T.R., 1984. A statistical exploration of the relationships of soil moisture characteristics to the physical properties of soils. Water Resour Res 20, 682–690. https://doi.org/10.1029/WR020i006p00682.
Dale, M.R.T., Fortin, M.-J., 2002. Spatial autocorrelation and statistical tests in ecology. Écoscience 9, 162–167. https://doi.org/10.1080/11956860.2002.11682702.
Dennison, P.E., Brewer, S.C., Arnold, J.D., Moritz, M.A., 2014. Large wildfire trends in the western United States, 1984-2011. Geophys. Res. Lett. 41, 2928–2933. https://doi.org/10.1002/2014GL059576.
Despain, D.G., 1990. Yellowstone vegetation: Consequences of Environment and History in a Natural Setting.
Despain, D.G., 1983. Nonpyrogenous climax lodgepole pine communities in Yellowstone National Park. Ecology 64, 231–234. https://doi.org/10.2307/1937070.
Emmett, K.D., Renwick, K.M., Poulter, B., 2019. Disentangling climate and disturbance effects on regional vegetation greening trends. Ecosystems 22, 873–891. https://doi.org/10.1007/s10021-018-0309-2.
Fischer, G., Nachtergaele, F., Prieler, S., van Velthuizen, H.T., Verelst, L., Wiberg, D., 2008. Global Agro-Ecological Zones Assessment for Agriculture (GAEZ 2008). IIASA, Laxenburg, Austria and FAO, Rome, Italy.
Fisher, R.A., Koven, C.D., Anderegg, W.R.L., Christoffersen, B.O., Dietze, M.C., Farrior, C. E., Holm, J.A., Hurtt, G.C., Knox, R.G., Lawrence, P.J., Lichstein, J.W., Longo, M., Matheny, A.M., Medvigy, D., Muller-Landau, H.C., Powell, T.L., Serbin, S.P., Sato, H., Shuman, J.K., Smith, B., Trugman, A.T., Viskari, T., Verbeeck, H., Weng, E., Xu, C., Xu, X., Zhang, T., Moorcroft, P.R., 2018. Vegetation demographics in Earth System Models: a review of progress and priorities. Glob Change Biol 24, 35–54. https://doi.org/10.1111/gcb.13910.
Flannigan, M.D., Krawchuk, M.A., de Groot, W.J., Wotton, B.M., Gowman, L.M., 2009. Implications of changing climate for global wildland fire. Int. J. Wildland Fire 18, 483. https://doi.org/10.1071/WF08187.
Friedlingstein, P., Jones, M.W., O'Sullivan, M., Andrew, R.M., Hauck, J., Peters, G.P., Peters, W., Pongratz, J., Sitch, S., Le Quéré, C., Bakker, D.C.E., Canadell, J.G., Ciais, P., Jackson, R.B., Anthoni, P., Barbero, L., Bastos, A., Bastrikov, V., Becker, M.,

Bopp, L., Buitenhuis, E., Chandra, N., Chevallier, F., Chini, L.P., Currie, K.I., Feely, R. A., Gehlen, M., Gilfillan, D., Gkritzalis, T., Goll, D.S., Gruber, N., Gutekunst, S., Harris, I., Haverd, V., Houghton, R.A., Hurtt, G., Ilyina, T., Jain, A.K., Joetzjer, E., Kaplan, J.O., Kato, E., Klein Goldewijk, K., Korsbakken, J.I., Landschützer, P., Lauvset, S.K., Lefèvre, N., Lenton, A., Lienert, S., Lombardozzi, D., Marland, G., McGuire, P.C., Melton, J.R., Metzl, N., Munro, D.R., Nabel, J.E.M.S., Nakaoka, S.-I., Neill, C., Omar, A.M., Ono, T., Peregon, A., Pierrot, D., Poulter, B., Rehder, G., Resplandy, L., Robertson, E., Rödenbeck, C., Séférian, R., Schwinger, J., Smith, N., Tans, P.P., Tian, H., Tilbrook, B., Tubiello, F.N., van der Werf, G.R., Wiltshire, A.J., Zaehle, S., 2019. Global Carbon Budget 2019. Earth Syst. Sci. Data 11, 1783–1838. https://doi.org/10.5194/essd-11-1783-2019.

Gavin, D.G., Fitzpatrick, M.C., Gugger, P.F., Heath, K.D., Rodríguez-Sánchez, F., Dobrowski, S.Z., Hampe, A., Hu, F.S., Ashcroft, M.B., Bartlein, P.J., Blois, J.L., Carstens, B.C., Davis, E.B., de Lafontaine, G., Edwards, M.E., Fernandez, M., Henne, P.D., Herring, E.M., Holden, Z.A., Kong, W., Liu, J., Magri, D., Matzke, N.J., McGlone, M.S., Saltré, F., Stigall, A.L., Tsai, Y.-H.E., Williams, J.W., 2014. Climate refugia: joint inference from fossil records, species distribution models and phylogeography. New Phytol 204, 37–54. https://doi.org/10.1111/nph.12929.

Gelaro, R., McCarty, W., Suárez, M.J., Todling, R., Molod, A., Takacs, L., Randles, C.A., Darmenov, A., Bosilovich, M.G., Reichle, R., Wargan, K., Coy, L., Cullather, R., Draper, C., Akella, S., Buchard, V., Conaty, A., da Silva, A.M., Gu, W., Kim, G.-K., Koster, R., Lucchesi, R., Merkova, D., Nielsen, J.E., Partyka, G., Pawson, S., Putman, W., Rienecker, M., Schubert, S.D., Sienkiewicz, M., Zhao, B., 2017. The Modern-Era Retrospective Analysis for Research and Applications, Version 2 (MERRA-2). J. Climate 30, 5419–5454. https://doi.org/10.1175/JCLI-D-16-0758.1.

Gillespie, A.J.R., 1999. Rationale for a national annual forest inventory program. J. For. 97, 16–20.

Hansen, A., Ireland, K., Legg, K., Keane, R., Barge, E., Jenkins, M., Pillet, M., 2016. Complex challenges of maintaining whitebark pine in greater Yellowstone under climate change: a call for innovative research, management, and policy approaches. Forests 7, 54. https://doi.org/10.3390/f7030054.

Hansen, A.J., Phillips, L.B., 2015. Which tree species and biome types are most vulnerable to climate change in the US Northern Rocky Mountains? For. Ecol. Manage. 338, 68–83. https://doi.org/10.1016/j.foreco.2014.11.008.

Hansen, W.D., Braziunas, K.H., Rammer, W., Seidl, R., Turner, M.G., 2018. It takes a few to tango: changing climate and fire regimes can cause regeneration failure of two subalpine conifers. Ecology 99, 966–977. https://doi.org/10.1002/ecy.2181.

Hansen, W.D., Turner, M.G., 2019. Origins of abrupt change? Postfire subalpine conifer regeneration declines nonlinearly with warming and drying. Ecol Monogr 89, e01340. https://doi.org/10.1002/ecm.1340.

Hantson, S., Arneth, A., Harrison, S.P., Kelley, D.I., Prentice, I.C., Rabin, S.S., Archibald, S., Mouillot, F., Arnold, S.R., Artaxo, P., Bachelet, D., Ciais, P., Forrest, M., Friedlingstein, P., Hickler, T., Kaplan, J.O., Kloster, S., Knorr, W., Lasslop, G., Li, F., Mangeon, S., Melton, J.R., Meyn, A., Sitch, S., Spessa, A., van der Werf, G.R., Voulgarakis, A., Yue, C., 2016. The status and challenge of global fire modelling. Biogeosciences 13, 3359–3375. https://doi.org/10.5194/bg-13-3359-2016.

Hantson, S., Kelley, D.I., Arneth, A., Harrison, S.P., Archibald, S., Bachelet, D., Forrest, M., Hickler, T., Lasslop, G., Li, F., Mangeon, S., Melton, J.R., Nieradzik, L., Rabin, S.S., Prentice, I.C., Sheehan, T., Sitch, S., Teckentrup, L., Voulgarakis, A., Yue, C., 2020. Quantitative assessment of fire and vegetation properties in simulations with fire-enabled vegetation models from the Fire Model Intercomparison Project. Geosci. Model Dev. 13, 3299–3318. https://doi.org/10.5194/gmd-13-3299-2020.

Harvey, B.J., Donato, D.C., Turner, M.G., 2016. High and dry: post-fire tree seedling establishment in subalpine forests decreases with post-fire drought and large stand-replacing burn patches: drought and post-fire tree seedlings. Global Ecol. Biogeogr. 25, 655–669. https://doi.org/10.1111/geb.12443.

Haxeltine, A., Prentice, I.C., 1996. BIOME3: an equilibrium terrestrial biosphere model based on ecophysiological constraints, resource availability, and competition among plant functional types. Global Biogeochem Cycles 10, 693–709.

Hickler, T., Smith, B., Sykes, M.T., Davis, M.B., Sugita, S., Walker, K., 2004. Using a generalized vegetation model to simulate vegetation dynamics in Northeastern USA. Ecology 85, 519–530. https://doi.org/10.1890/02-0344.

Hickler, T., Vohland, K., Feehan, J., Miller, P.A., Smith, B., Costa, L., Giesecke, T., Fronzek, S., Carter, T.R., Cramer, W., Kühn, I., Sykes, M.T., 2012. Projecting the future distribution of European potential natural vegetation zones with a generalized, tree species-based dynamic vegetation model: future changes in European vegetation zones. Glob. Ecol. Biogeography 21, 50–63. https://doi.org/10.1111/j.1466-8238.2010.00613.x.

Higuera, P.E., Whitlock, C., Gage, J.A., 2011. Linking tree-ring and sediment-charcoal records to reconstruct fire occurrence and area burned in subalpine forests of Yellowstone National Park, USA. Holocene 21, 327–341. https://doi.org/10.1177/0959683610374882.

Hijmans, R.J., 2019. raster: Geographic Data Analysis and Modeling.

Holling, C.S., 1973. Resilience and Stability of Ecological Systems. Annu Rev Ecol Syst 1–23.

Iglesias, V., Krause, T.R., Whitlock, C., 2015. Complex response of white pines to past environmental variability increases understanding of future vulnerability. PLoS ONE 10, e0124439. https://doi.org/10.1371/journal.pone.0124439.

Jönsson, A.M., Schroeder, L.M., Lagergren, F., Anderbrant, O., Smith, B., 2012. Guess the impact of Ips typographus—An ecosystem modelling approach for simulating spruce bark beetle outbreaks. Agric For Meteorol 166-167, 188–200. https://doi.org/10.1016/j.agrformet.2012.07.012.

Kashian, D.M., Romme, W.H., Tinker, D., Turner, M.G., Ryan, M.G., 2012. Data from: post-fire changes in forest carbon storage over a 300-year chronosequence of Pinus contorta-dominated forests. Dryad. Digital Repository. 10.5061/dryad.1v87f.

Kashian, D.M., Romme, W.H., Tinker, D.B., Turner, M.G., Ryan, M.G., 2013. Postfire changes in forest carbon storage over a 300-year chronosequence of Pinus contorta -dominated forests. Ecol Monogr 83, 49–66. https://doi.org/10.1890/11-1454.1.

Kashian, D.M., Romme, W.H., Tinker, D.B., Turner, M.G., Ryan, M.G., 2006. Carbon storage on landscapes with stand-replacing Fires. Bioscience 56, 598. https://doi.org/10.1641/0006-3568(2006)56[598:CSOLWS]2.0.CO;2.

Kasischke, E.S., Turetsky, M.R., 2006. Recent changes in the fire regime across the North American boreal region—Spatial and temporal patterns of burning across Canada and Alaska. Geophys. Res. Lett. 33, L09703. https://doi.org/10.1029/2006GL025677.

Keane, R.E., 2019. Applying Ecosystem and Landscape Models in Natural Resource Management. CRC Press, Boca Raton.

Keane, R.E., Garner, J.L., Schmidt, K.M., Long, D.G., Menakis, J.P., Finney, M.A., 1998. Development of Input Data Layers for the FARSITE Fire Growth Model for the Selway-Bitterroot Wilderness Complex, USA (General Technical Report No. RMRS-GTR-3). U.S. Department of Agriculture, Forest Service, Rocky Mountain Research Station, Ogden, UT.

Keane, R.E., Loehman, R.A., Holsinger, L.M., 2011. The FireBGCv2 Landscape Fire and Succession model: a Research Simulation Platform For Exploring Fire and Vegetation Dynamics (General Technical Report No. RMRS-GTR-255). U.S. Department of Agriculture, Forest Service, Rocky Mountain Research Station, Ft. Collins, CO. https://doi.org/10.2737/RMRS-GTR-255.

Keane, Robert E., McKenzie, Donald, Falk, Donald A., Smithwick, Erica A.H., Miller, Carol, Kellogg, Lara-Karena B., 2015. Representing climate, disturbance, and vegetation interactions in landscape models. Ecological Modelling 309-310, 33–47. https://doi.org/10.1016/j.ecolmodel.2015.04.009.

Keane, R.E., Reinhardt, E.D., Scott, J., Gray, K., Reardon, J., 2005. Estimating forest canopy bulk density using six indirect methods. Can. J. For. Res. 35, 724–739. https://doi.org/10.1139/x04-213.

Keeley, J.E., 2009. Fire intensity, fire severity and burn severity: a brief review and suggested usage. Int. J. Wildland Fire 18, 116. https://doi.org/10.1071/WF07049.

Kelley, D.I., Prentice, I.C., Harrison, S.P., Wang, H., Simard, M., Fisher, J.B., Willis, K.O., 2013. A comprehensive benchmarking system for evaluating global vegetation models. Biogeosciences 10, 3313–3340. https://doi.org/10.5194/bg-10-3313-2013.

Koca, D., Smith, B., Sykes, M.T., 2006. Modelling regional climate change effects on potential natural ecosystems in Sweden. Climatic Change 78, 381–406. https://doi.org/10.1007/s10584-005-9030-1.

Kottek, M., Grieser, J., Beck, C., Rudolf, B., Rubel, F., 2006. World Map of the Köppen-Geiger climate classification updated. Meteorologische Zeitschrift 15, 259–263. https://doi.org/10.1127/0941-2948/2006/0130.

Lay, E.H., 2004. WWLL global lightning detection system: regional validation study in Brazil. Geophys. Res. Lett. 31, L03102. https://doi.org/10.1029/2003GL018882.

Le Quéré, C., Andrew, R.M., Friedlingstein, P., Sitch, S., Hauck, J., Pongratz, J., Pickers, P.A., Korsbakken, J.I., Peters, G.P., Canadell, J.G., Arneth, A., Arora, V.K., Barbero, L., Bastos, A., Bopp, L., Chevallier, F., Chini, L.P., Ciais, P., Doney, S.C., Gkritzalis, T., Goll, D.S., Harris, I., Haverd, V., Hoffman, F.M., Hoppema, M., Houghton, R.A., Hurtt, G., Ilyina, T., Jain, A.K., Johannessen, T., Jones, C.D., Kato, E., Keeling, R.F., Goldewijk, K.K., Landschützer, P., Lefèvre, N., Lienert, S., Liu, Z., Lombardozzi, D., Metzl, N., Munro, D.R., Nabel, J.E.M.S., Nakaoka, S., Neill, C., Olsen, A., Ono, T., Patra, P., Peregon, A., Peters, W., Peylin, P., Pfeil, B., Pierrot, D., Poulter, B., Rehder, G., Resplandy, L., Robertson, E., Rocher, M., Rödenbeck, C., Schuster, U., Schwinger, J., Séférian, R., Skjelvan, I., Steinhoff, T., Sutton, A., Tans, P.P., Tian, H., Tilbrook, B., Tubiello, F.N., van der Laan-Luijkx, I.T., van der Werf, G.R., Viovy, N., Walker, A.P., Wiltshire, A.J., Wright, R., Zaehle, S., Zheng, B., 2018. Global carbon budget 2018. Earth Syst. Sci. Data 10, 2141–2194. https://doi.org/10.5194/essd-10-2141-2018.

Lehsten, V., Arneth, A., Spessa, A., Thonicke, K., Moustakas, A., 2016. The effect of fire on tree–grass coexistence in savannas: a simulation study. Int. J. Wildland Fire 25, 137. https://doi.org/10.1071/WF14205.

Li, F., Zeng, X.D., Levis, S., 2012. A process-based fire parameterization of intermediate complexity in a Dynamic Global Vegetation Model. Biogeosciences 9, 2761–2780. https://doi.org/10.5194/bg-9-2761-2012.

Li, F., Val Martin, M., Andreae, M.O., Arneth, A., Hantson, S., Kaiser, J.W., Lasslop, G., Yue, C., Bachelet, D., Forrest, M., Kluzek, E., Liu, X., Mangeon, S., Melton, J.R., Ward, D.S., Darmenov, A., Hickler, T., Ichoku, C., Magi, B.I., Sitch, S., van der Werf, G.R., Wiedinmyer, C., Rabin, S.S., 2019. Historical (1700–2012) global multi-model estimates of the fire emissions from the Fire Modeling Intercomparison Project (FireMIP). Atmos. Chem. Phys. 19, 12545–12567. https://doi.org/10.5194/acp-19-12545-2019.

Littell, J.S., 2002. Determinants of Fire Regime Variability in Lower Elevation Forests of the Northern Greater Yellowstone Ecosystem (PhD Dissertation). Montana State University.

Litton, C.M., Ryan, M.G., Tinker, D.B., Knight, D.H., 2003. Belowground and aboveground biomass in young postfire lodgepole pine forests of contrasting tree density. Can. J. For. Res. 33, 16.

Manabe, S., 1969. The atmospheric circulation and the hydrology of the earth's surface. Monthly Weather Rev. 97, 739–774.

McCaughey, W.W., Schmidt, W.C., 2001. Taxonomy, distribution, and history. Whitebark Pine Communities: Ecology and Restoration. Island Press.

McCaughey, W.W., Schmidt, W.C., Schmidt, W., C., McDonald, K.athy J., 1990. Autecology of whitebark pine. compilers Proceedings–symposium On Whitebark Pine ecosystems: Ecology and Management of a High-Mountain Resource; 1989 March 29-31; Bozeman, MT. (General Technical Report No. INT-270). U.S.

Department of Agriculture, Forest Service, Intermountain Research Station, Ogden, UT.
McDowell, N., Barnard, H., Bond, B., Hinckley, T., Hubbard, R., Ishii, H., Köstner, B., Magnani, F., Marshall, J., Meinzer, F., Phillips, N., Ryan, M., Whitehead, D., 2002. The relationship between tree height and leaf area: sapwood area ratio. Oecologia 132, 12–20. https://doi.org/10.1007/s00442-002-0904-x.
Miller, D.A., White, R.A., 1998. A conterminous United States multilayer soil characteristics dataset for regional climate and hydrology modeling. Earth Interact. 2, 1–26.
Mladenoff, D.J., 2004. LANDIS and forest landscape models. Ecol Modell 180, 7–19. https://doi.org/10.1016/j.ecolmodel.2004.03.016.
Moorcroft, P.R., Hurtt, G.C., Pacala, S.W., 2001. A method for scaling vegetation dynamics: the ecosystem demography model (ED). Ecol Monogr 71, 29.
Morales, P., Hickler, T., Rowell, D.P., Smith, B., Sykes, M.T., 2007. Changes in European ecosystem productivity and carbon balance driven by regional climate model output. Global Change Biol. 13, 108–122. https://doi.org/10.1111/j.1365-2486.2006.01289.x.
MTBS Data Access: Fire Level Geospatial Data, 2017. MTBS Project (USDA Forest Service/U.S. Geological Survey). Available online: http://mtbs.gov/direct-download [July 2018].
Notaro, M., Emmett, K., O'Leary, D., 2019. Spatio-temporal variability in remotely sensed vegetation greenness across Yellowstone National Park. Remote Sens (Basel) 11, 798. https://doi.org/10.3390/rs11070798.
Oyler, J.W., Ballantyne, A., Jencso, K., Sweet, M., Running, S.W., 2015. Creating a topoclimatic daily air temperature dataset for the conterminous United States using homogenized station data and remotely sensed land skin temperature. Int. J. Climatol 35, 2258–2279. https://doi.org/10.1002/joc.4127.
Penman, J., Gytarsky, M., Hiraishi, T., Krug, T., Kruger, D., Pipatti, R., Buendia, L., Miwa, K., Ngara, T., Tanabe, K., Wagner, F., 2003. Good Practice Guidance For Land Use, Land-Use Change and Forestry. Institute for Global Environmental Strategies, Kanagawa Prefecture, Japan.
Pfeiffer, M., Spessa, A., Kaplan, J.O., 2013. A model for global biomass burning in preindustrial time: LPJ-LMfire (v1.0). Geosci Model Dev. 6, 643–685. https://doi.org/10.5194/gmd-6-643-2013.
Piekielek, N.B., Hansen, A.J., Chang, T., 2016. Past, Present, and future impacts of climate on the vegetation communities of the greater Yellowstone ecosystem across elevation gradients. In: Hansen, A.J., Monahan, W.B., Olliff, S.T., Theobald, D.M. (Eds.), Climate Change in Wildlands. Island Press/Center for Resource Economics, Washington, DC, pp. 190–211. https://doi.org/10.5822/978-1-61091-713-1_10.
Pierce, D., 2017. ncdf4: Interface to Unidata netCDF (Version 4 Or Earlier) Format Data Files. R package version 1.16, https://CRAN.R-project.org/package=ncdf4.
Potter, C., 2019. Changes in vegetation cover of Yellowstone National Park estimated from MODIS Greenness Trends, 2000 to 2018. Remote Sens Earth Syst Sci 2, 147–160. https://doi.org/10.1007/s41976-019-00019-5.
Potter, C., Klooster, S., Crabtree, R., Huang, S., Gross, P., Genovese, V., 2011. Carbon fluxes in ecosystems of Yellowstone National Park predicted from remote sensing data and simulation modeling. Carbon Balance Manage 6, 3. https://doi.org/10.1186/1750-0680-6-3.
Poulter, B., Frank, D.C., Hodson, E.L., Zimmermann, N.E., 2011. Impacts of land cover and climate data selection on understanding terrestrial carbon dynamics and the CO₂ airborne fraction. Biogeosciences 8, 2027–2036. https://doi.org/10.5194/bg-8-2027-2011.
Prentice, I.C., Leemans, R., 1990. Pattern and process and the dynamics of forest structure: a simulation approach. The Journal of Ecology 78 (2), 340–355. https://doi.org/10.2307/2261116.
Pugh, T.A.M., Arneth, A., Kautz, M., Poulter, B., Smith, B., 2019a. Important role of forest disturbances in the global biomass turnover and carbon sinks. Nat. Geosci. 12, 730–735. https://doi.org/10.1038/s41561-019-0427-2.
Pugh, T.A.M., Lindeskog, M., Smith, B., Poulter, B., Arneth, A., Haverd, V., Calle, L., 2019b. Role of forest regrowth in global carbon sink dynamics. Proc Natl Acad Sci USA 116, 4382–4387. https://doi.org/10.1073/pnas.1810512116.
Rabin, S.S., Melton, J.R., Lasslop, G., Bachelet, D., Forrest, M., Hantson, S., Kaplan, J.O., Li, F., Mangeon, S., Ward, D.S., Yue, C., Arora, V.K., Hickler, T., Kloster, S., Knorr, W., Nieradzik, L., Spessa, A., Folberth, G.A., Sheehan, T., Voulgarakis, A., Kelley, D.I., Prentice, I.C., Sitch, S., Harrison, S., Arneth, A., 2017. The Fire Modeling Intercomparison Project (FireMIP), phase 1: experimental and analytical protocols with detailed model descriptions. Geosci. Model Dev. 10, 1175–1197. https://doi.org/10.5194/gmd-10-1175-2017.
Reinhardt, E.D., Keane, R.E., Brown, J.K., 1997. First Order Fire Effects Model: FOFEM 4.0, User's Guide (No. INT-GTR-344). U.S. Department of Agriculture, Forest Service, Intermountain Research Station, Ogden, UT. https://doi.org/10.2737/INT-GTR-344.
Reinhardt, E.D., Lutes, D.C., Scott, J., 2006. FuelCalc: a Method for Estimating Fuel Characteristics (RMRS-P No. 41). comps. In: Andrews, P.atricia L., Butler,, B.ret W. (Eds.), 2006. Fuels Management—How to Measure Success: Conference Proceedings. 28-30 March 2006; Portland, OR. Proceedings RMRS-P-41. Fort Collins, CO: U.S. Department of Agriculture, Forest Service, Rocky Mountain Research Station.
Renkin, R.A., Despain, D.G., 1992. Fuel moisture, forest type, and lightning-caused fire in Yellowstone National Park. Can. J. For. Res. 22, 37–45. https://doi.org/10.1139/x92-005.
Rodman, A.W., Shovic, H.F., Thoma, D.P., 1996. Soils of Yellowstone National Park. Yellowstone Center for Resources, National Park Service.
Romme, W.H., 1982. Fire and landscape diversity in subalpine forests of Yellowstone National Park. Ecol Monogr 52, 199–221. https://doi.org/10.2307/1942611.
Romme, W.H., Despain, D.G., 1989. Historical Perspective on the Yellowstone Fires of 1988. Bioscience 39, 695–699. https://doi.org/10.2307/1311000.
Rothermel, R.C., 1972. A Mathematical Model For Predicting Fire Spread in Wildland Fuels (Research Paper INT-115). USDA Forest Service.
RStudio Team, 2016. RStudio: Integrated Development Environment for R. RStudio, Inc., Boston, MA.
Santantonio, D., Hermann, R.K., Overton, W.S., 1977. Root biomass studies in forest ecosystems. Pedobiologia (Jena) 17, 1–31.
Santoro, M., 2018. GlobBiomass - Global Datasets of Forest biomass. PANGAEA. 10.1594/PANGAEA.894711.
Schoennagel, T., Turner, M.G., Romme, W.H., 2003. The influence of fire interval and serotiny on postfire lodgepole pine density in Yellowstone National Park. Ecology 84, 2967–2978. https://doi.org/10.1890/02-0277.
Schulzweida, U., 2019. CDO user guide (Version 1.9.6).
Scott, J.H., Burgan, R.E., 2005. Standard Fire Behavior Fuel models: a Comprehensive Set For Use With Rothermel's Surface Fire Spread Model (No. RMRS-GTR-153). U.S. Department of Agriculture, Forest Service, Rocky Mountain Research Station, Ft. Collins, CO. https://doi.org/10.2737/RMRS-GTR-153.
Scott, J.H., Reinhardt, E.D., 2001. Assessing Crown Fire Potential By Linking Models of Surface and Crown Fire Behavior (No. RMRS-RP-29). U.S. Department of Agriculture, Forest Service, Rocky Mountain Research Station, Ft. Collins, CO. https://doi.org/10.2737/RMRS-RP-29.
Seidl, R., Rammer, W., Scheller, R.M., Spies, T.A., 2012. An individual-based process model to simulate landscape-scale forest ecosystem dynamics. Ecol Modell 231, 87–100. https://doi.org/10.1016/j.ecolmodel.2012.02.015.
Shanahan, E., Irvine, K.M., Thoma, D., Wilmoth, S., Ray, A., Legg, K., Shovic, H., 2016. Whitebark pine mortality related to white pine blister rust, mountain pine beetle outbreak, and water availability. Ecosphere 7, e01610. https://doi.org/10.1002/ecs2.1610.
Shinozaki, K., Yoda, K., Hozumi, K., Kira, T., 1964a. A quantitative analysis of the plant form - the pipe model theory I. Basic analyses. Japanese Journal of Ecology 14.
Shinozaki, K., Yoda, K., Hozumi, K., Kira, T., 1964b. A quantitative analysis of plant form - the pipe model theory II. Further evidence of the theory and its application in forest ecology. Jpn. J. Ecol. 10, 7.
Shmida, A., Ellner, S., 1984. Coexistence of plant species with similar niches. Vegetatio 58, 29–55.
Sitch, S., Smith, B., Prentice, I.C., Arneth, A., Bondeau, A., Cramer, W., Kaplan, J.O., Levis, S., Lucht, W., Sykes, M.T., Thonicke, K., Venevsky, S., 2003. Evaluation of ecosystem dynamics, plant geography and terrestrial carbon cycling in the LPJ dynamic global vegetation model. Global Change Biol 9, 161–185. https://doi.org/10.1046/j.1365-2486.2003.00569.x.
Smith, B., Knorr, W., Widlowski, J.-L., Pinty, B., Gobron, N., 2008. Combining remote sensing data with process modelling to monitor boreal conifer forest carbon balances. For. Ecol. Manage. 255, 3985–3994. https://doi.org/10.1016/j.foreco.2008.03.056.
Smith, B., Prentice, I.C., Sykes, M.T., 2001. Representation of vegetation dynamics in the modelling of terrestrial ecosystems: comparing two contrasting approaches within European climate space. Global Ecology and Biogeography 25.
Stephens, S.L., Burrows, N., Buyantuyev, A., Gray, R.W., Keane, R.E., Kubian, R., Liu, S., Seijo, F., Shu, L., Tolhurst, K.G., van Wagtendonk, J.W., 2014. Temperate and boreal forest mega-fires: characteristics and challenges. Front Ecol Environ 12, 115–122. https://doi.org/10.1890/120332.
Tang, G., Beckage, B., Smith, B., 2012. The potential transient dynamics of forests in New England under historical and projected future climate change. Climatic Change 114, 357–377. https://doi.org/10.1007/s10584-012-0404-x.
Tang, J., Zhuang, Q., 2008. Equifinality in parameterization of process-based biogeochemistry models: a significant uncertainty source to the estimation of regional carbon dynamics. J. Geophys. Res. 113 https://doi.org/10.1029/2008JG000757.
Thonicke, K., Spessa, A., Prentice, I.C., Harrison, S.P., Dong, L., Carmona-Moreno, C., 2010. The influence of vegetation, fire spread and fire behaviour on biomass burning and trace gas emissions: results from a process-based model. Biogeosciences 7, 1991–2011. https://doi.org/10.5194/bg-7-1991-2010.
Thonicke, K., Venevsky, S., Sitch, S., Cramer, W., 2001. The role of fire disturbance for global vegetation dynamics: coupling fire into a Dynamic Global Vegetation Model. Global Ecol. Biogeography 17.
Thornton, P.E., Thornton, M.M., Mayer, B.W., Wei, Y., Devarakonda, R., Vose, R.S., Cook, R.B., 2017. Daymet: Daily Surface Weather Data on a 1-km Grid for North America, Version 3. ORNL Distributed Active Archive Center. https://doi.org/10.3334/ORNLDAAC/1328.
Turner, M.G., Braziunas, K.H., Hansen, W.D., Harvey, B.J., 2019. Short-interval severe fire erodes the resilience of subalpine lodgepole pine forests. Proc Natl Acad Sci USA 116, 11319–11328. https://doi.org/10.1073/pnas.1902841116.
Turner, M.G., Hargrove, W.W., Gardner, R.H., Romme, W.H., 1994. Effects of fire on landscape heterogeneity in Yellowstone National Park, Wyoming. J. Vegetation Sci. 5, 731–742. https://doi.org/10.2307/3235886.
Turner, M.G., Romme, W.H., Gardner, R.H., Hargrove, W.W., 1997. Effects of fire size and pattern on early succession in Yellowstone National Park. Ecol Monogr 67, 411–433. https://doi.org/10.1890/0012-9615(1997)067[0411:EOFSAP]2.0.CO;2.
Turner, M.G., Tinker, D.B., Romme, W.H., Kashian, D.M., Litton, C.M., 2004. Landscape patterns of sapling density, leaf area, and aboveground net primary production in postfire lodgepole pine forests, Yellowstone National Park (USA). Ecosystems 7, 751–775. https://doi.org/10.1007/s10021-004-0011-4.
Turner, M.G., Whitby, T.G., Tinker, D.B., Romme, W.H., 2017. Data from: twenty-four years after the Yellowstone fires: are postfire lodgepole pine stands converging in structure and function? Dryad Dataset. 10.5061/dryad.1pr7k.

Turner, M.G., Whitby, T.G., Tinker, D.B., Romme, W.H., 2016. Twenty-four years after the Yellowstone Fires: are postfire lodgepole pine stands converging in structure and function. Ecology 97, 1260–1273. https://doi.org/10.1890/15-1585.1.

U.S. DOE, 2018. Disturbance and Vegetation Dynamics in Earth System Models; Workshop Report, DOE/SC-0196. Office of Biological and Environmental Research, U.S. Department of Energy Office of Science.

Van Wagner, C.E., 1993. Prediction of crown fire behavoir in two stands of jack pine. Can. J. For. Res. 23, 442–449.

Van Wagner, C.E., 1977. Conditions for the start and spread of crown fire. Can. J. For. Res. 7, 23–34.

Van Wagner, C.E., 1973. Height of Crown Scorch in Forest Fires. Can. J. For. Res. 3.

Walker, X.J., Baltzer, J.L., Cumming, S.G., Day, N.J., Ebert, C., Goetz, S., Johnstone, J.F., Potter, S., Rogers, B.M., Schuur, E.A.G., Turetsky, M.R., Mack, M.C., 2019. Increasing wildfires threaten historic carbon sink of boreal forest soils. Nature 572, 520–523. https://doi.org/10.1038/s41586-019-1474-y.

Weaver, T., 2001. Whitebark pine and its environment. Whitebark Pine Communities: Ecology and Restoration. Island, Washington, DC, pp. 41–72.

Westerling, A.L., 2016. Increasing western US forest wildfire activity: sensitivity to changes in the timing of spring. Phil. Trans. R. Soc. B 371, 20150178. https://doi.org/10.1098/rstb.2015.0178.

Westerling, A.L., 2006. Warming and earlier spring increase Western U.S. forest wildfire activity. Science 313, 940–943. https://doi.org/10.1126/science.1128834.

Westerling, A.L., Turner, M.G., Smithwick, E.A.H., Romme, W.H., Ryan, M.G., 2011. Continued warming could transform Greater Yellowstone fire regimes by mid-21st century. Proc Natl Acad Sci USA 108, 13165–13170. https://doi.org/10.1073/pnas.1110199108.

White, A., Cannell, M.G.R., Friend, A.D., 2000. The high-latitude terrestrial carbon sink: a model analysis. Global Change Biol 6, 227–245. https://doi.org/10.1046/j.1365-2486.2000.00302.x.

Whitlock, C., Shafer, S.L., Marlon, J., 2003. The role of climate and vegetation change in shaping past and future fire regimes in the northwestern US and the implications for ecosystem management. For. Ecol. Manage. 178, 5–21. https://doi.org/10.1016/S0378-1127(03)00051-3.

Wilson, M.V., Botkin, D.B., 1990. Models of simple microcosms: emergent properties and the effect of complexity on stability. Am. Nat. 135, 414–434. https://doi.org/10.1086/285054.

Zaehle, S., Sitch, S., Prentice, I.C., Liski, J., Cramer, W., Erhard, M., Hickler, T., Smith, B., 2006. The importance of age-related decline in forest NPP for modeling regional carbon balances. Ecol. Appl. 16, 1555–1574. https://doi.org/10.1890/1051-0761(2006)016[1555:TIOADI]2.0.CO;2.

Zender, C.S., 2014. netCDF operator (NCO) user guide, Version 4.4.3.

Zhu, D., Peng, S.S., Ciais, P., Viovy, N., Druel, A., Kageyama, M., Krinner, G., Peylin, P., Ottlé, C., Piao, S.L., Poulter, B., Schepaschenko, D., Shvidenko, A., 2015. Improving the dynamics of Northern Hemisphere high-latitude vegetation in the ORCHIDEE ecosystem model. Geosci. Model Dev. 8, 2263–2283. https://doi.org/10.5194/gmd-8-2263-2015.

Zhu, Z., Piao, S., Myneni, R.B., Huang, M., Zeng, Z., Canadell, J.G., Ciais, P., Sitch, S., Friedlingstein, P., Arneth, A., Cao, C., Cheng, L., Kato, E., Koven, C., Li, Y., Lian, X., Liu, Y., Liu, R., Mao, J., Pan, Y., Peng, S., Peñuelas, J., Poulter, B., Pugh, T.A.M., Stocker, B.D., Viovy, N., Wang, X., Wang, Y., Xiao, Z., Yang, H., Zaehle, S., Zeng, N., 2016. Greening of the earth and its drivers. Nat. Clim. Change 6, 791–795. https://doi.org/10.1038/nclimate3004.